

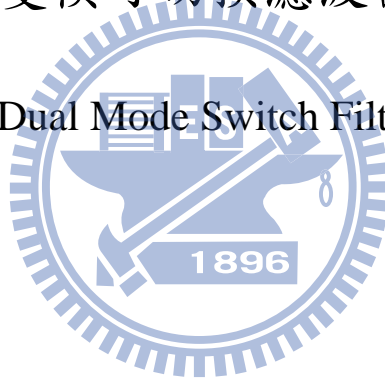
# 國立交通大學

電機學院通訊與網路科技產業研發碩士班

## 碩士論文

雙模可切換濾波器

Dual Mode Switch Filter



研究生：廖德裕

指導教授：張志揚 教授

中華民國一百年一月

雙頻可切換濾波器  
Dual Mode Switch Filter


研究生：廖德裕

Student : Te-Yu Liao

指導教授：張志揚

Advisor : Dr. Chi-Yang Chang

國立交通大學  
電機學院通訊與網路科技產業研發碩士班  
碩士論文



A Thesis  
Submitted to College of Electrical and Computer Engineering  
National Chiao Tung University  
in partial Fulfillment of the Requirements  
for the Degree of  
Master  
in

Industrial Technology R & D Master Program on  
Communication Engineering

Jan 2011

Hsinchu, Taiwan, Republic of China

中華民國一〇一一年一月

# 雙模可切換濾波器

研究生：廖德裕

指導教授：張志揚博士

國立交通大學電機學院產業研發碩士班

## 摘 要

本論文提出一個中心頻率為 2.5GHz 的雙模可切換濾波器。此電路為對稱的結構，利用二極體順向偏壓及逆向偏壓的切換來改變濾波器的特性，使得在二極體順向偏壓時只有共模信號可通過電路而奇模信號則會被阻絕，在二極體逆向偏壓時則反之。

本論文的研製主要由帶通濾波器的設計開始，並將二極體及電容的特性參數帶入，設計出等效的半電路，其次進行帶止濾波器及全止濾波器的分析，接著將這些等效的半電路轉換為對稱結構的電路，即可取得此雙模可切換濾波器的架構。此論文中電路的工作頻帶為 2.4GHz~2.6GHz，並且以微帶線製作在介電常數 3.58、厚度為 20mil 的 RO4003 的基板上。

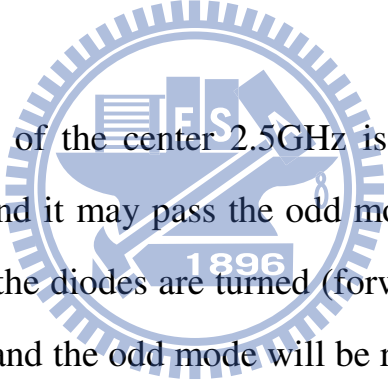
# Dual Mode Switch Filter

Student: Te-Yu Liao

Advisor: Dr. Chi-Yang Chang

Industrial Technology R & D Master Program of  
Electrical and Computer Engineering College  
National Chiao Tung University

## Abstract



A switching circuit of the center 2.5GHz is proposed in this thesis. The circuit is symmetrical, and it may pass the odd mode signal and reject the even signal or vice versa. As the diodes are turned (forward bias), the even mode can pass through the circuit and the odd mode will be rejected. On the other hand, as the diodes turned off (reverse bias), the situation reversed.

Firstly, we design the band-pass filter and take the characteristic of the components into consideration, and then we may analyze the performance of the band-stop filter and the all-stop filter. Combining these half circuits (2 band-pass filters, 1 band-stop filter, 1 all-stop filter), we may get the whole structure of the switching circuit. The whole circuit in this thesis is operated in 2.4GHz~2.6GHz. It is fabricated with microstrip line on a RO4003 substrate with a dielectric constant of 3.58, a thickness of 20 mil.

# Acknowledgement

## 誌謝

時間過得真快，兩年的研究所生活在轉眼間就要結束了。在此要感謝很多貴人的幫助，讓我能夠順利完成學業及論文。

首先要感謝我的指導教授張志揚博士。在老師的諄諄教誨和耐心指導之下，我學習到許多微波領域相關的知識，並且得以應用在研究之上。當遇到研究上的難題，老師也都會指引方向，讓我得以解決克服這些難關。平常在校與老師一同吃飯的時候，也感受到老師的身教。在此由衷地感謝您。同時，我要感謝在論文口試時給予我許多寶貴建議的口試委員鍾世忠教授、林育德教授，本論文也因此得以更加完善。

接下來，我要感謝 916 實驗室的學長姐、同學、以及學弟妹。博士班學長益廷、正憲、昀緯在平日的課業和研究上，給予我許多的指點，可說是我在課堂之外的小老師。其餘的學長姐、同學、學弟妹的陪伴，使得整個實驗室充滿歡樂的氣氛，也讓我在學習和研究都充滿動力。其中包括已畢業的學長姐哲慶、宗傑、殿靖、如屏、揚達、聖智、嫻潔、士峰、耿宏，博士班學長建育，以及同學維欣、懿萱、鵬達、宛蓉。我也要感謝曾經一同修課的同學們，謝謝你們的一路相伴。

此外，我要感謝和碩的主管鄭光志副總，因為您的鼓勵，我才會報考產碩專班、完成碩士的學業。我也要感謝我的直屬主管吳瑞欽副理，以及部門的同事們，因為你們的支持及協助，我才能在工作之餘順利地完成學業。

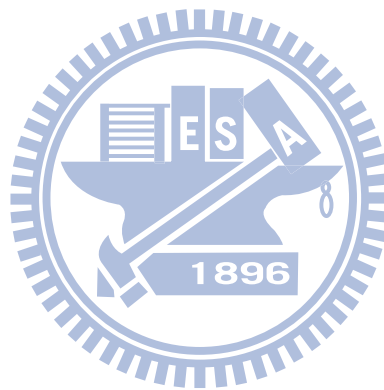
最後，我要感謝我最愛的老婆召琴，這兩年照顧兒子浩辰、以及對我的包容及鼓勵，讓我可以在工作及課業上沒有後顧之憂。我要感謝我的父母親及妹妹，感謝你們的支持與陪伴，讓我能夠順利的完成碩士學位，謝謝你們！

# Tables of Contents

Abstract(Chinese).....	i
Abstract.....	ii
Acknowledgement.....	iii
Table of Contents.....	iv
List of Tables.....	v
List of Figures.....	vi
Chapter 1 Introduction.....	1
Chapter 2 The Circuit Description and Design Flow.....	3
2.1 Dual Mode Switch Filter Circuits Analysis.....	3
2.2 Filter Specifications and Design Flow.....	6
Chapter 3 Microwave Filter Theorem.....	17
3.1 Reflection Coefficient and Input Impedance.....	17
3.2 S-Parameters.....	18
3.3 Equal Ripple Filter.....	23
3.4 Impedance and Frequency Scaling.....	24
3.5 Band-pass and Band-Stop Transformation.....	26
3.6 Impedance and Admittance Inverters.....	28
3.7 Band-stop and Band-pass Filters Using Quarter-Wave Resonators.....	33
Chapter 4 Circuit Implementation.....	38
4.1 Chebyshev Low-pass Filter.....	38
4.2 Band-pass Filter.....	38
4.3 Band-stop Filter.....	44
4.4 All-stop Filter.....	47
Chapter 5 Fabrication and Measurements.....	50
5.1 Circuit Fabrication.....	50
5.2 Measurement and 3D EM Simulation Correlation.....	51
5.3 Conclusion.....	53
References.....	55

## List of Tables

Table 2.1: The summary of 4 operation modes of the dual mode switch filter .....	5
Table 2.2: The component parameters of the lumped circuits .....	6
Table 2.3: The ideal transmission line parameters of the dual mode switch filter .....	7
Table 2.4: The parameters of the PCB .....	8
Table 2.5: The physical parameters of the microstrip line or the microstrip coupled line of the filter .....	8
Table 4.1: The elements of low-pass prototype filter of return loss -17dB .....	38
Table 4.2: The elements of low-pass prototype filter of return loss -17dB .....	40



## List of Figures

Figure 1.1: The block diagram of the duplexer .....	1
Figure 2.1: The description of the dual mode switch filter .....	3
Figure 2.2: The circuit of the dual mode switch filter for diode on and odd mode.....	3
Figure 2.3: The simplified half circuit of the dual mode switch filter for diode on and odd mode .....	4
Figure 2.4: The circuit of the dual mode switch filter for diode on and even mode .....	4
Figure 2.5: The simplified half circuit of the dual mode switch filter for diode on and even mode .....	4
Figure 2.6: The circuit of the dual mode switch filter for diode off and odd mode .....	4
Figure 2.7: The simplified half circuit of the dual mode switch filter for diode off and odd mode .....	5
Figure 2.8: The circuit of the dual mode switch filter for diode off and even mode.....	5
Figure 2.9: The simplified half circuit of the dual mode switch filter for diode off and even mode .....	5
Figure 2.10: Simulated insertion loss of the dual mode switch filter (with ideal transmission line).....	7
Figure 2.11: Simulated return loss of the dual mode switch filter (with ideal transmission line) .....	8
Figure 2.12: The circuit of the dual mode switch filter for diode on (with microstrip line) ...	9
Figure 2.13: The circuit of the dual mode switch filter for diode off (with microstrip line)...	9
Figure 2.14: Simulated insertion loss of the dual mode switch filter (with microstrip line). ..	10
Figure 2.15: Simulated return loss of the dual mode switch filter (with microstrip line) .....	10
Figure 2.16: The layout and the dimensions of the dual mode switch filter .....	11
Figure 2.17: 3D EM simulated insertion loss of the dual mode switch filter.....	11
Figure 2.18: 3D EM simulated return loss of the dual mode switch filter .....	12
Figure 2.19: 3D EM simulated insertion loss when diode resistance changes.....	12
Figure 2.20: 3D EM simulated return loss when diode resistance changes .....	13
Figure 2.21: 3D EM simulated insertion loss when diode capacitance changes .....	13
Figure 2.22: 3D EM simulated return loss when diode capacitance changes .....	14
Figure 2.23: 3D EM simulated insertion loss when diode inductance changes .....	14
Figure 2.24: 3D EM simulated return loss when diode inductance changes.....	15
Figure 2.25: 3D EM simulated insertion loss when diode resistance, capacitance, and inductance change.....	15
Figure 2.26: 3D EM simulated return loss when diode resistance, capacitance, and inductance change.....	16



Figure 3.1: Transmission line circuit for mismatched load and generator .....	18
Figure 3.2: An arbitrary N-port microwave network.....	19
Figure 3.3: A two-port coupled line filter section.....	21
Figure 3.4: (a)Low-pass prototype (b)Transformation to band-pass filter (c)Transformation to band-stop filter .....	26
Figure 3.5: Summary of prototype filter transformation .....	28
Figure 3.6: Impedance and admittance inverters (a)Operation of impedance and admittance inverters (b)Impedance as quarter-wave transformation .....	28
Figure 3.7: Impedance and admittance inverters.....	29
Figure 3.8: Impedance inverter.....	30
Figure 3.9: Impedance and admittance inverters.....	31
Figure 3.10: Impedance and admittance inverters.....	32
Figure 3.11: Impedance scaling of the K inverter .....	32
Figure 3.12: Admittance scaling of the J inverter.....	33
Figure 3.13: Impedance scaling of the K inverter.....	33
Figure 3.14: Band-stop and band-pass filters using shunt transmission line resonators ( $\theta = \pi/2$ at the center frequency) (a)Band-stop filter (b)Band-pass filter.....	34
Figure 3.15: Equivalent circuit for the band-stop filter. (a)Equivalent circuit of open-circuited stub for $\theta$ near $\pi/2$ (b)Equivalent filter circuit using resonators and admittance inverter (c)Equivalent lumped-element band-stop filter.....	35
Figure 4.1: Band-pass filter of return loss 17dB, center frequency 2.5GHz, fractional bandwidth 15%.....	39
Figure 4.2: Simulated insertion loss and return loss of the band-pass filter in figure 4.1 .....	39
Figure 4.3: Impedance and admittance inverters.....	40
Figure 4.4: Admittance scaling of the J inverter.....	40
Figure 4.5: Band-pass filter of return loss 17dB, center frequency 2.5GHz, fractional bandwidth 15%.....	40
Figure 4.6: Simulated insertion loss and return loss of the band-pass filter in figure 4.5 .....	41
Figure 4.7: Band-pass filter of return loss 17dB, center frequency 2.5GHz, fractional bandwidth 15%.....	42
Figure 4.8: Simulated insertion loss and return loss the band-pass filter in figure 4.7 .....	42
Figure 4.9: Band-pass filter of return loss 17dB, center frequency 2.5GHz, fractional bandwidth 15%.....	43
Figure 4.10: Simulated insertion loss and return loss of the band-pass filter in figure 4.9... ..	43
Figure 4.11: Band-pass filter of return loss 17dB, center frequency 2.5GHz, fractional bandwidth 15%.....	44
Figure 4.12: Simulated insertion loss and return loss of the band-pass filter in figure 4.11 .....	44
Figure 4.13: Band-stop filter under diode off, even mode, with insertion loss >35dB .....	45

Figure 4.14: Simulated insertion loss and return loss of the band-stop filter in figure 4.13	.45
Figure 4.15: Band-pass filter under diode on, even mode, with return loss >15dB	.....45
Figure 4.16: Simulated insertion loss and return loss of the band-pass filter in figure 4.15	.46
Figure 4.17: Band-pass filter under diode off, odd mode, with return loss >15dB	.....46
Figure 4.18: Simulated insertion loss and return loss of the band-pass filter in figure 4.17	.47
Figure 4.19: All-stop filter	.....47
Figure 4.20: All-stop filter under diode on, odd mode, with insertion loss >35dB	.....48
Figure 4.21: Simulated insertion loss and return loss of the all-pass filter in figure 4.20	.....49
Figure 5.1: Photograph of the dual mode switch filter	.....50
Figure 5.2: Measured insertion loss of dual mode switch filter	.....51
Figure 5.3: Measured return loss of dual mode switch filter	.....51
Figure 5.4: Measurement and 3D EM simulation correlation under diode on / odd mode	...52
Figure 5.5: Measurement and 3D EM simulation correlation under diode on / even mode	.52
Figure 5.6: Measurement and 3D EM simulation correlation under diode off / odd mode	..53
Figure 5.7: Measurement and 3D EM simulation correlation under diode off / even mode	.53
.....	



# Chapter 1 Introduction

Odd mode and even mode analysis is usually applied in symmetrical microwave circuits. Odd mode is that the input pair has the same magnitude but 180 degrees phase difference. Recently, differential signal becomes more and more popular because it shows better immunity against the crosstalk. Moreover, modern RF integrated circuit using differential design is the trend.

A switching circuit is proposed in this thesis to pass the odd mode signal and reject the even mode or vice versa. As the diodes are turned on (forward bias), the even mode can pass through the circuit and the odd mode will be rejected. On the other hand, as the diodes are turned off (reverse bias), the situation reversed. The odd mode signal can be changed to the even mode signal if we apply an 180° phase shifter on one of the signal path. Similarly, the even mode signal can also be changed to odd mode signal. Therefore the proposed circuit can select wanted signal to pass. Figure 1.1 shows a balanced duplexer, applying the proposed circuit can enhance the T/R channel isolation.

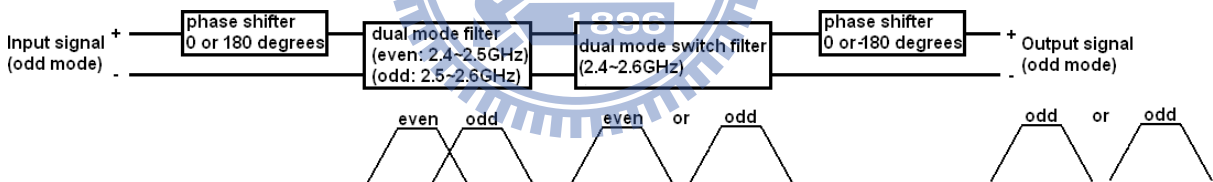


Figure 1.1 The block diagram of the duplexer

In Chapter 2, we will analyze the even mode and odd mode circuits for diodes on and off and introduce the design flow. The performance impact due to component variance is also discussed in this chapter.

In Chapter 3, basic microwave theories related to the proposed circuits are introduced. These theories will be used in the dual mode switch filter design and analysis. Reflection coefficient, input impedance, and S-parameter, are the bases in microwave circuits analysis and design. The impedance approximation of the coupled line will be used to analysis of DC blocking circuits which is used in the I/O portion of the proposed circuit. Equal ripple filter, impedance and frequency scaling, band-pass and band-stop transformation will be used in this filter

design to get better bandwidth. Impedance and admittance inverters will be used to convert the lumped elements to the line or the coupled line, which is useful in circuit implementation. Band-pass and band-stop filter using quarter-wave resonators will be useful in circuit implementation as well.

In Chapter 4, the circuits analysis and the proto-type filter design flow will be introduced. By analyzing the sub-system, the filter performance will be analyzed in simplified equivalent circuits.

In Chapter 5, the measurement result and the correlation between the simulation and the measurement will be referred. It is confirmed that the dual-mode switch filter is fabrication achievable as well.



## Chapter 2 The Circuit Description and Design Flow

### 2.1 Dual Mode Switch Filter Circuits Analysis

The odd mode and the even mode are often used in filter application. We use the diodes as the “switches”, so that we may decide which mode to “go through” the filter by turning on (forward bias) or turning off (reverse bias) the diodes. When the diodes are on, only the even mode signal will be transmitted; when the diodes are off, only the odd mode signal will be transmitted.

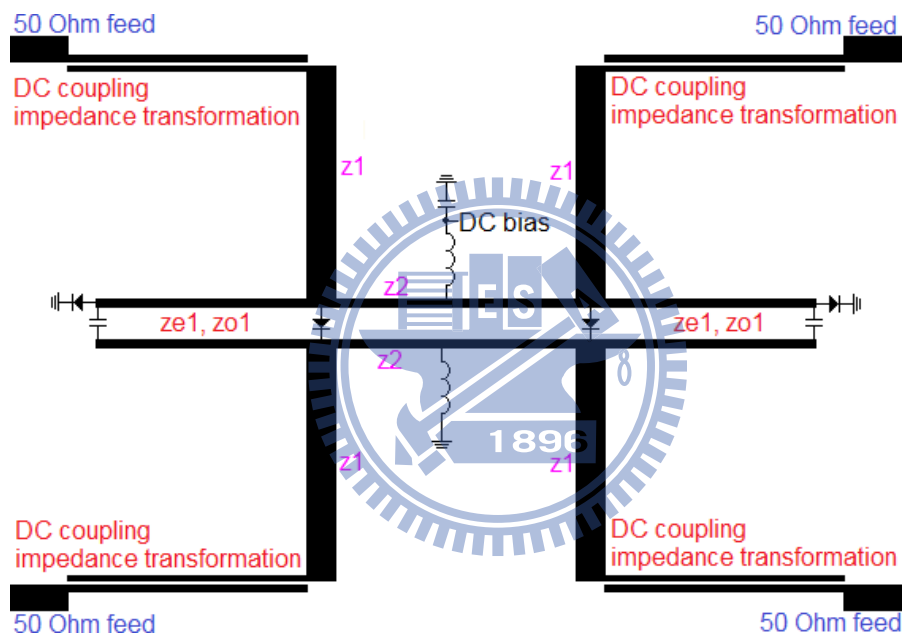


Figure 2.1 The description of the dual mode switch filter

Since the upper half and the lower half circuits are symmetrical, we may analyze the circuits with equivalent half circuit for both even and odd modes. For diodes on, the equivalent half circuit of the odd mode looks like an all-stop filter.

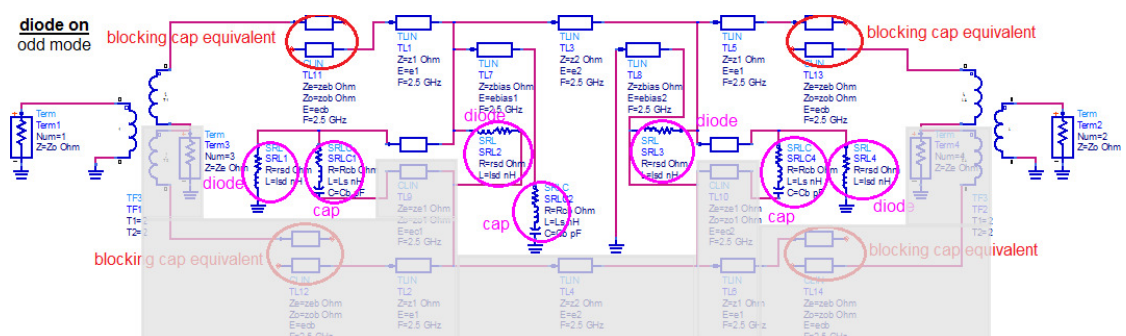


Figure 2.2 The circuit of the dual mode switch filter for diode on and odd mode

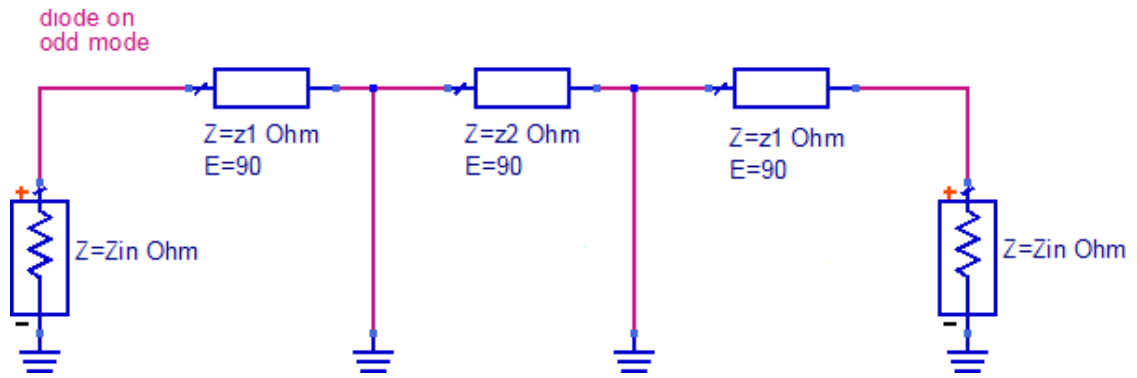


Figure 2.3 The simplified half circuit of the dual mode switch filter for diode on and odd mode

For diodes on, the even mode half circuit looks like a band-pass filter.

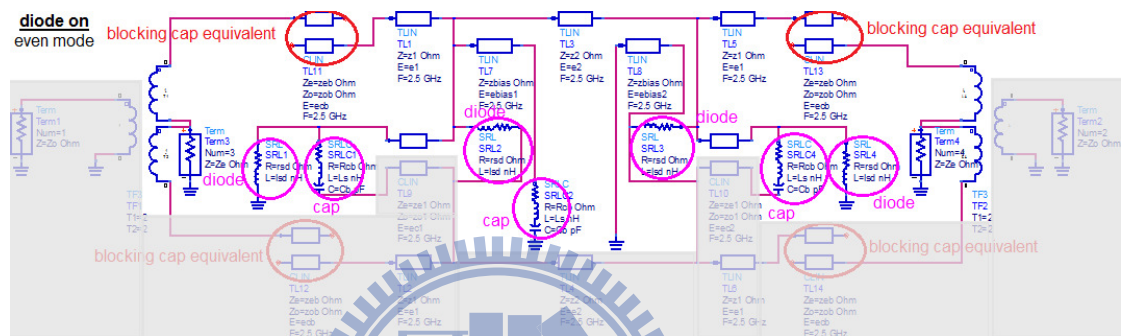


Figure 2.4 The circuit of the dual mode switch filter for diode on and even mode

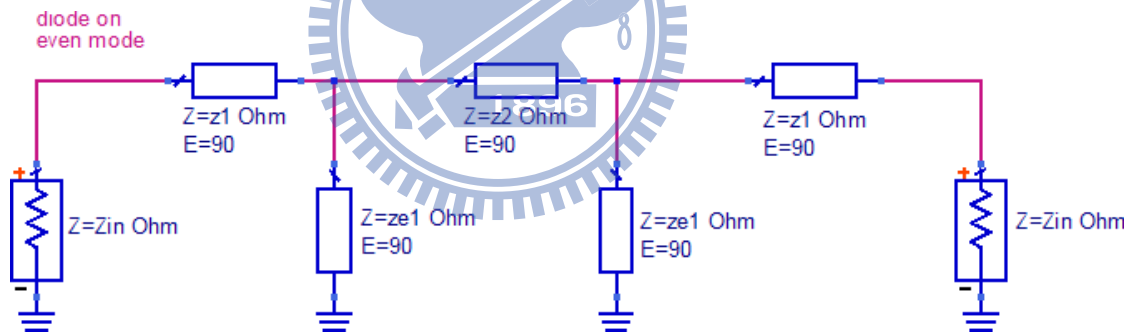


Figure 2.5 The simplified half circuit of the dual mode switch filter for diode on and even mode

For diodes off, the odd mode half circuit looks like a band-pass filter.

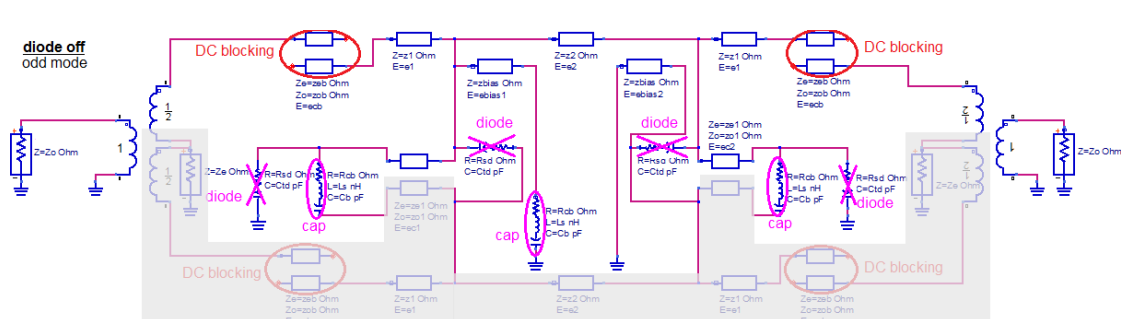


Figure 2.6 The circuit of the dual mode switch filter for diode off and odd mode

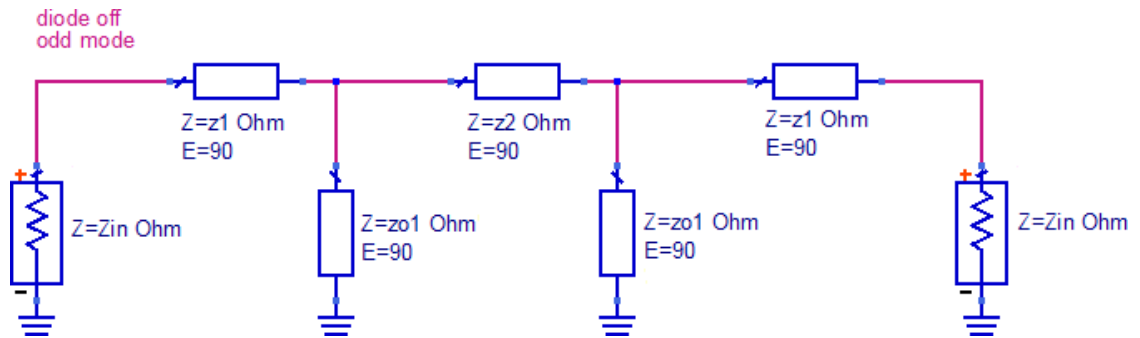


Figure 2.7 The simplified half circuit of the dual mode switch filter for diode off and odd mode

For diodes off, the even mode half circuit looks like a band-stop filter.

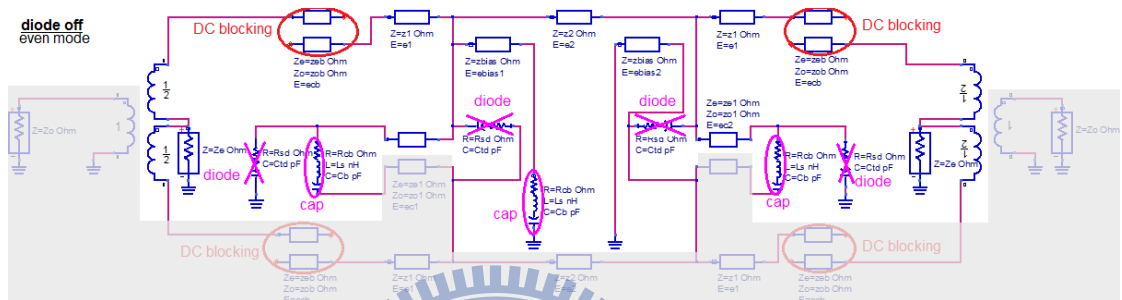


Figure 2.8 The circuit of the dual mode switch filter for diode off and even mode

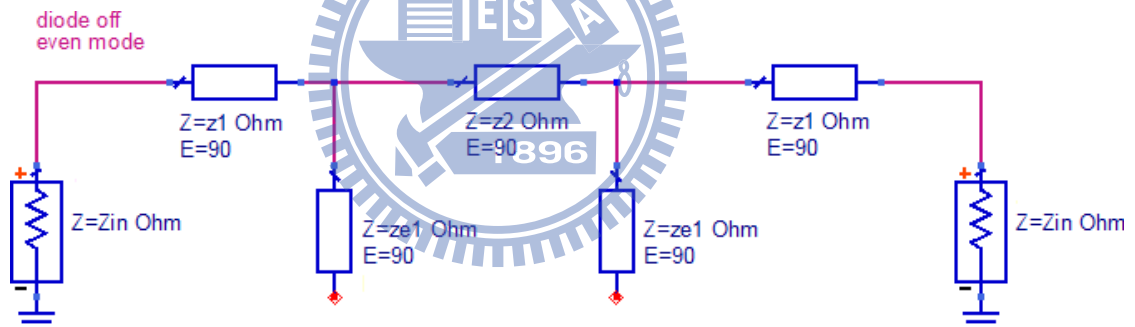
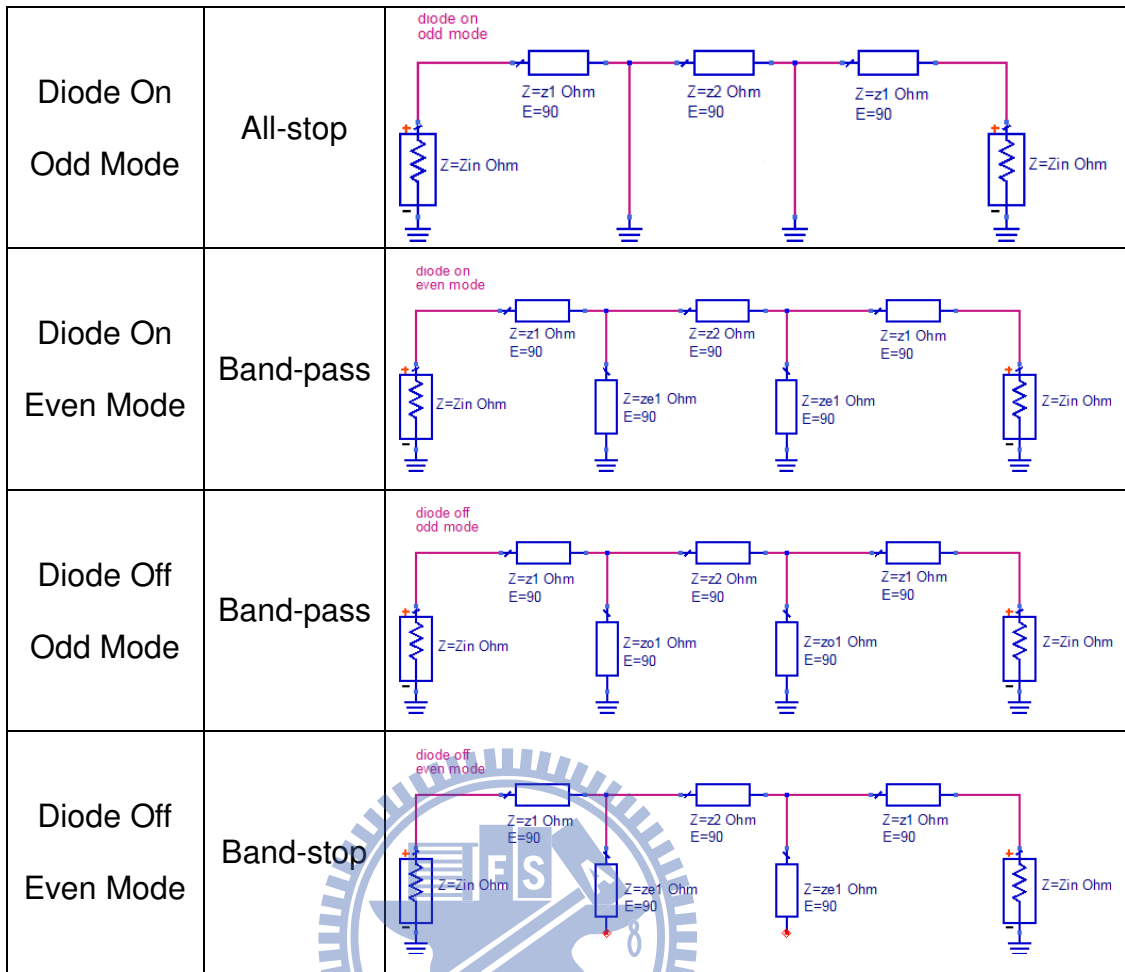


Figure 2.9 The simplified half circuit of the dual mode switch filter for diode off and even mode

If we provide a positive DC bias voltage via DC bias circuit, the diodes are turned on, otherwise the diodes are off. At the operation frequency, the bias choke is equivalent to an open circuit, which will not affect the filter performance. The blocking capacitor ( $C_b$ ) passes the RF signal and blocks the DC voltage.

Table 2.1 The summary of 4 operation modes of the dual mode switch filter

Circuit Type	Filter Type	Equivalent Half Circuit
--------------	-------------	-------------------------



## 2.2 Filter Specifications and Design Flow

The target bandwidth is 2.4GHz~2.6GHz. The target insertion loss of the pass-band is <3dB, and the target insertion loss of the stop-band is >35dB. The target return loss of the pass-band is >15dB, and the target return loss of the stop-band is <3dB.

Followings are the parameters of the circuit components.

Table 2.2 The component parameters of the lumped circuits

Zo (Ohm)	Ze (Ohm)	Blocking cap. Cb (pF)	Series resistance of the Cb Rcb (Ohm)	Series inductance of the Cb Ls (nH)
100	25	10	0.559	0.5
Diode forward resistance rsd (Ohm)	Diode series inductance lsd (nH)	Diode reverse resistance Rsd (Ohm)	Diode reverse capacitance Ctd (pF)	



3.14	0.4	3.14	0.06	
------	-----	------	------	--

We can get the parameters of the circuits as below after circuit optimization.

Table 2.3 The ideal transmission line parameters of the dual mode switch filter

z1 (Ohm)	e1 (degrees)	z2 (Ohm)	e2 (degrees)	ze1 (Ohm)
45.9159	89.1999	83.7614	83.4545	92.0885
zo1 (Ohm)	ec1(degrees)	ec2(degrees)	zbias (Ohm)	ebias1(degrees)
83.9994	82.7498	93.0212	100.491	99.0715
ebias2(degrees)	zeb (Ohm)	zob (Ohm)	ecb(degrees)	
75.2906	130.62	64.9333	90.4566	

Below are the simulation results of the insertion loss and the return loss. The bandwidth (pass-band insertion loss <3dB, stop-band insertion loss >35dB, pass-band return loss >15dB, stop-band return loss <3dB) is 2.305GHz~2.693GHz.

### Insertion loss

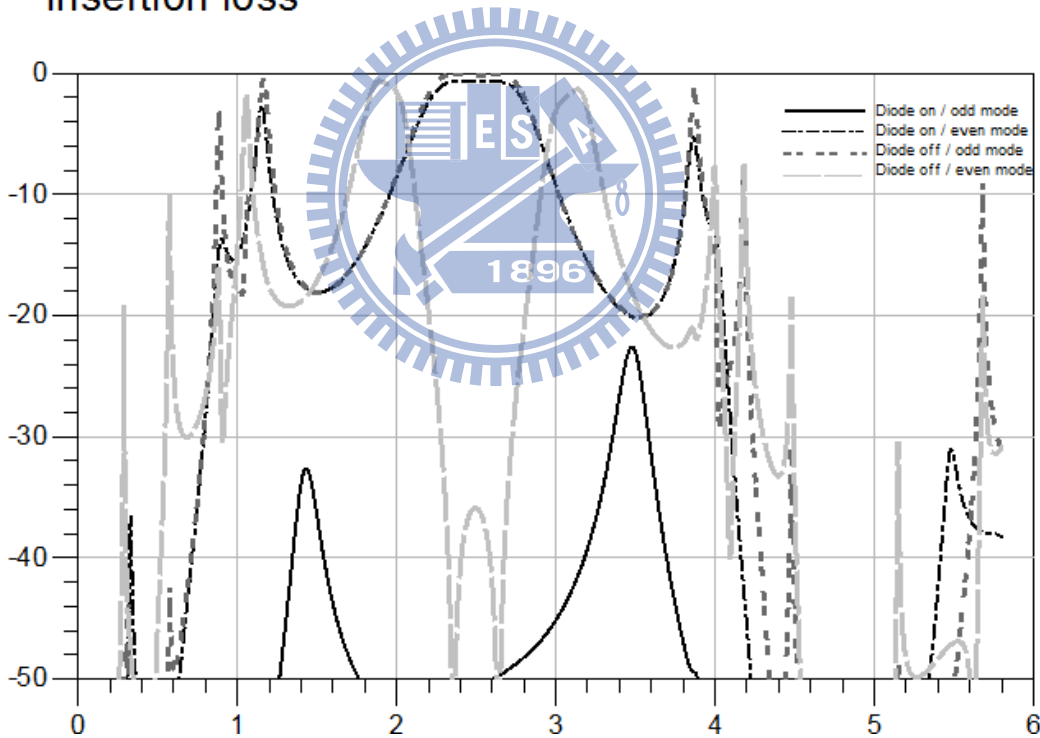


Figure 2.10 Simulated insertion loss of the dual mode switch filter (with ideal transmission line)

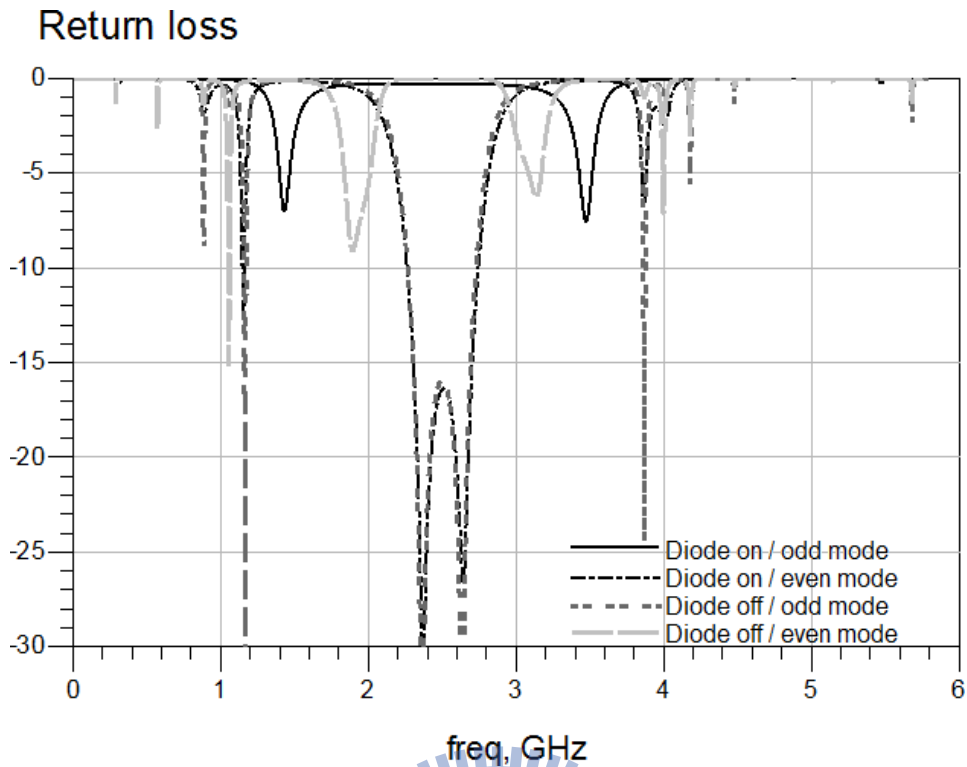


Figure 2.11 Simulated return loss of the dual mode switch filter (with ideal transmission line)

Table 2.3 shows the ideal transmission line impedance and electrical length of the filter. The PCB parameters are listed in table 2.4. Then, we may calculate the line width, length, and spacing of the microstrip line or microstrip coupled line.

Table 2.4 The parameters of the PCB

Center freq. $f_0$ (GHz)	Dielectric thickness H (mil)	Dielectric constant $\epsilon_r$
2.5	20	3.58
Dielectric loss tangent	Metal thickness T (mil)	Metal conductivity (S/m)
$2.7 \cdot 10^{-3}$	0.7	$5.8 \cdot 10^7$

Table 2.5 shows the calculated line width, spacing, and length of the corresponding transmission line. It also shows the physical parameters of microstrip line and microstrip coupled line after circuit optimization.

Table 2.5 The physical parameters of the microstrip line or the microstrip coupled line of the filter

	w1 (mil)	l1 (mil)	w2 (mil)	l2 (mil)	wc1 (mil)
Calculated	50	697	16	682	14

Fine tuned	50	616	16	841	14
	sc1 (mil)	lc1 (mil)	lc2 (mil)	wbias (mil)	lbias1 (mil)
Calculated	58	677	761	10	821
Fine tuned	60	661	743	12	740
	lbias2 (mil)	wb (mil)	sb (mil)	lb (mil)	
Calculated	624	10	8	761	
Fine tuned	572	10	8	773	

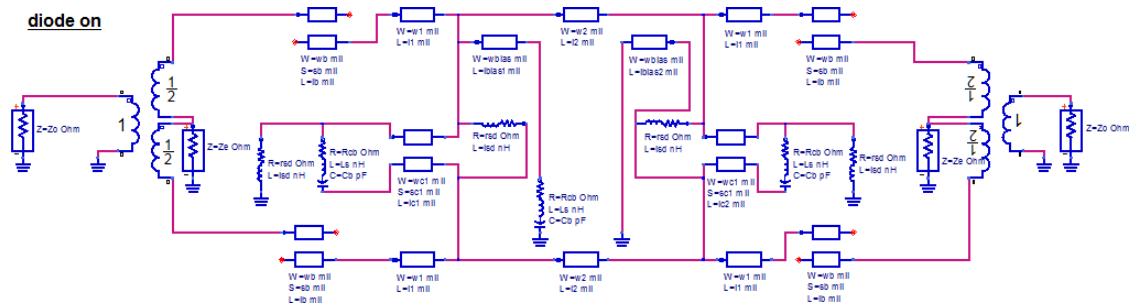


Figure 2.12 The circuit of the dual mode switch filter for diode on (with microstrip line)

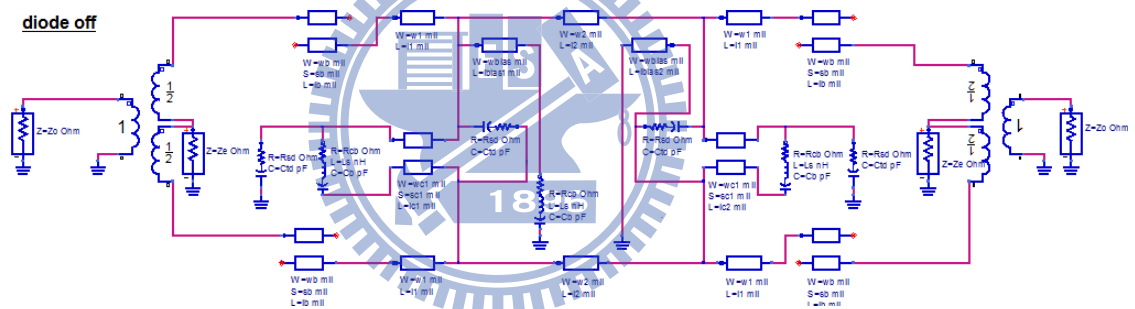


Figure 2.13 The circuit of the dual mode switch filter for diode off (with microstrip line)

Followings are the simulated results of the insertion loss and the return loss based on microstrip model. The bandwidth (pass-band insertion loss <3dB, stop-band insertion loss >35dB, pass-band return loss >15dB, stop-band return loss <3dB) is 2.306GHz~2.697GHz.

## Insertion loss

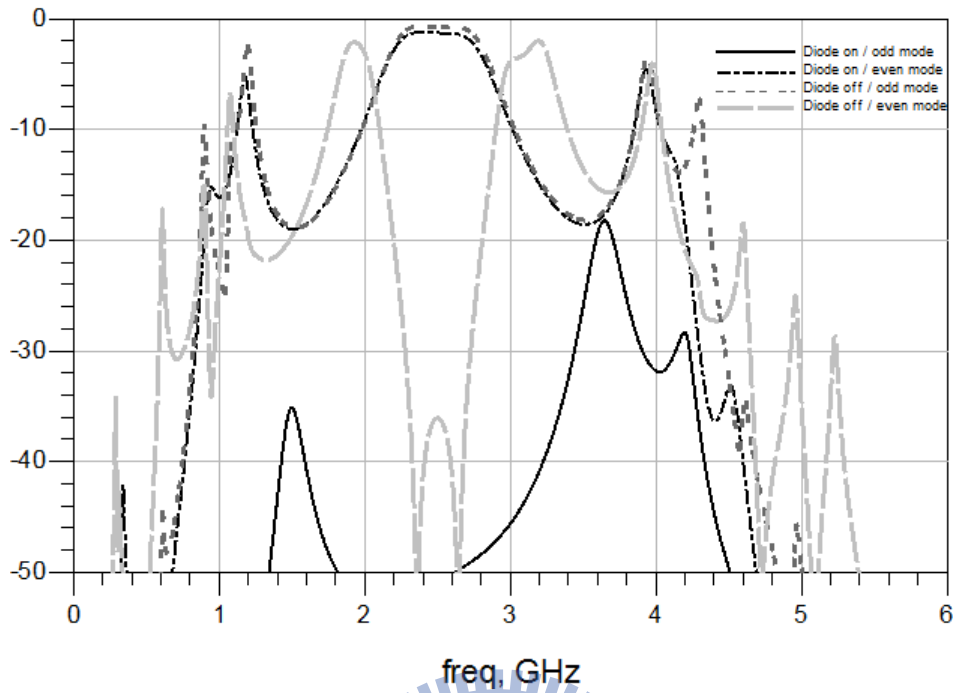


Figure 2.14 Simulated insertion loss of the dual mode switch filter (with microstrip line)

## Return loss

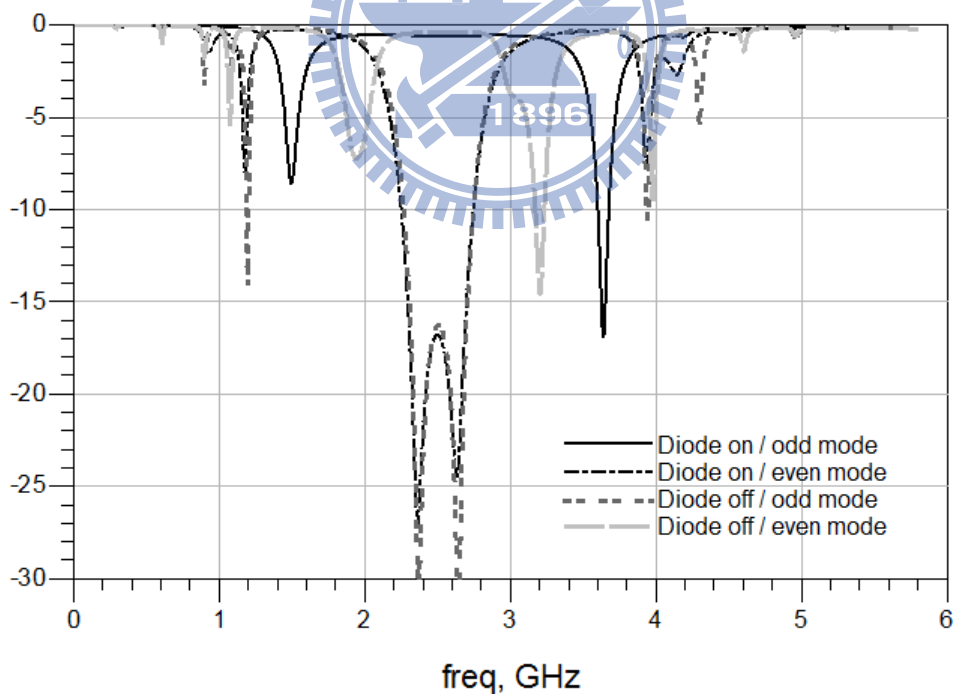


Figure 2.15 Simulated return loss of the dual mode switch filter (with microstrip line)

In order to minimize the PCB size of the circuits, we make use of Meander lines. The circuit simulator could take the junction effect and the coupling effect between the lines into account. Due to these effects, we need to fine tune the trace length of each

transmission line to get a better fit to the specifications. The layout is shown as below.

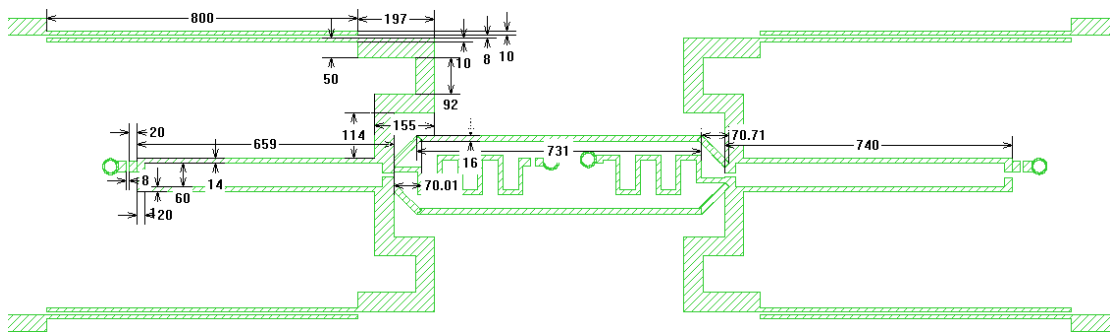


Figure 2.16 The layout and the dimensions of the dual mode switch filter

Followings are the insertion loss and the return loss of EM simulation. The bandwidth (pass-band insertion loss  $<3\text{dB}$ , stop-band insertion loss  $>34.785\text{dB}$ , pass-band return loss  $>14.271\text{dB}$ , stop-band return loss  $<3\text{dB}$ ) is  $2.344\text{GHz}\sim 2.654\text{GHz}$ . The return loss does not meet the design spec, but it is still higher than  $10\text{dB}$ .

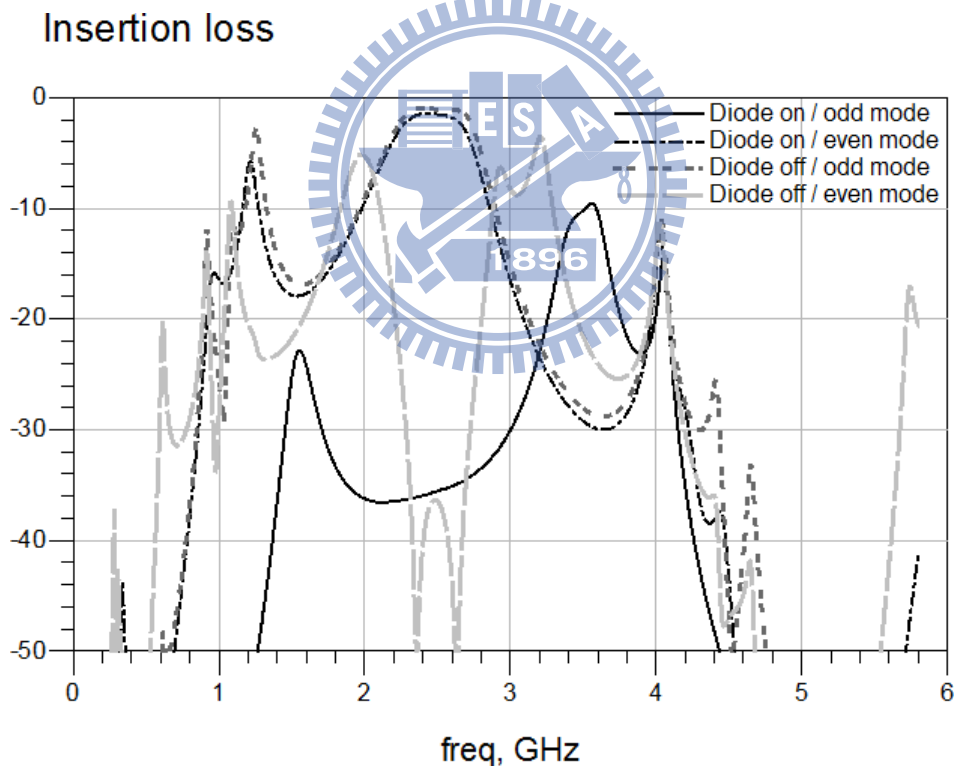


Figure 2.17 3D EM simulated insertion loss of the dual mode switch filter

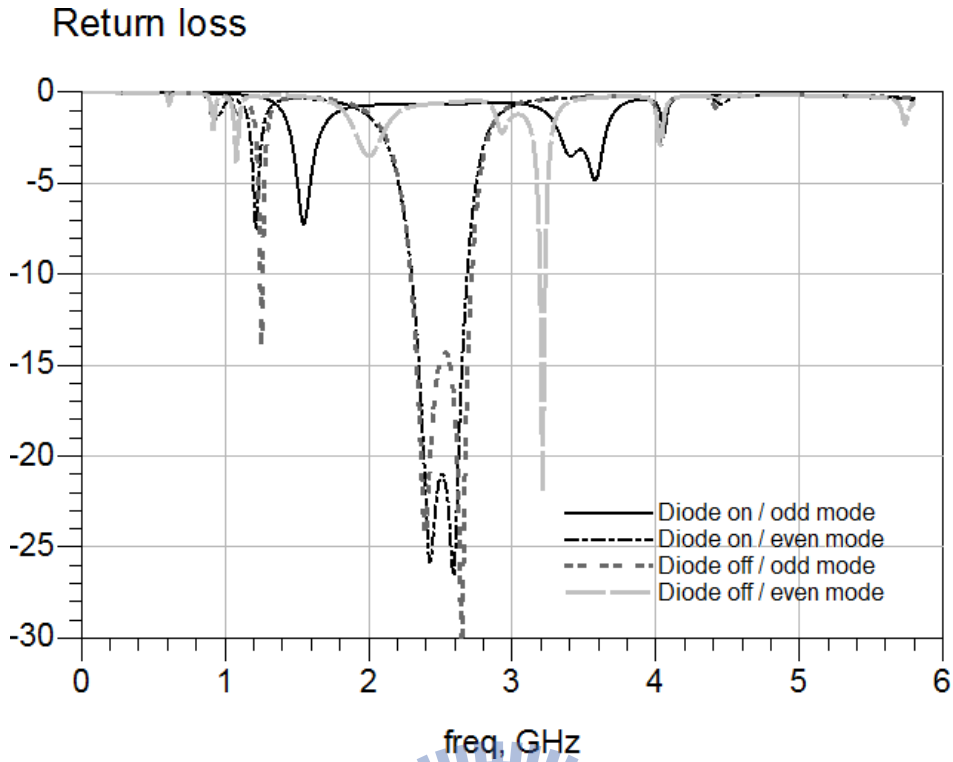


Figure 2.18 3D EM simulated return loss of the dual mode switch filter

The filter performance will be degraded if the component parameters are changed. If the resistance of the diodes is changed from 3.14 Ohm to 3.50 Ohm or to 2.50 Ohm, the filter performance keeps almost unchanged, and the bandwidth (pass-band insertion loss <3dB, stop-band insertion loss >34.758dB, pass-band return loss >14.271dB, stop-band return loss <3dB) is still 2.344GHz~2.654GHz.

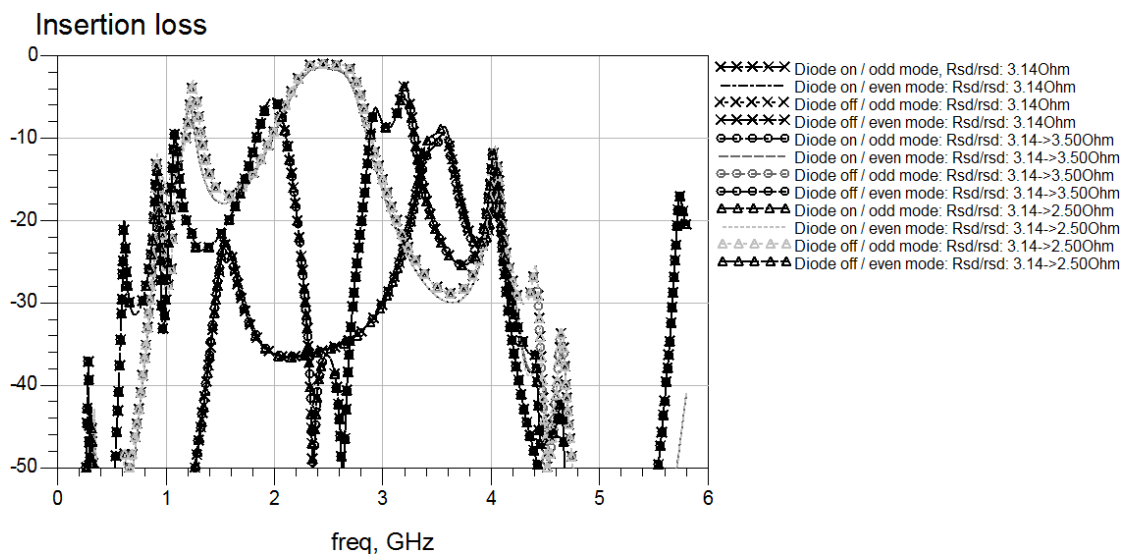


Figure 2.19 3D EM simulated insertion loss when diode resistance changes

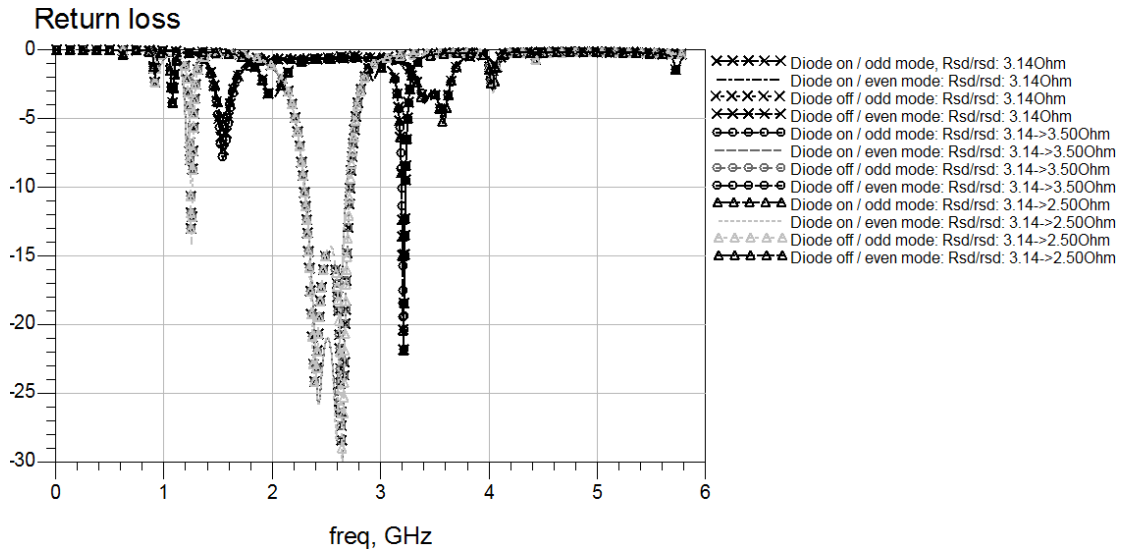


Figure 2.20 3D EM simulated return loss when diode resistance changes

If the capacitance of the diodes is changed from 0.06pF to 0.18pF or to 0.03pF, there will be a frequency shift, and the bandwidth (pass-band insertion loss <3dB, stop-band insertion loss >35dB, pass-band return loss >13.167dB, stop-band return loss <3dB) will be decreased to 2.339GHz~2.543GHz.

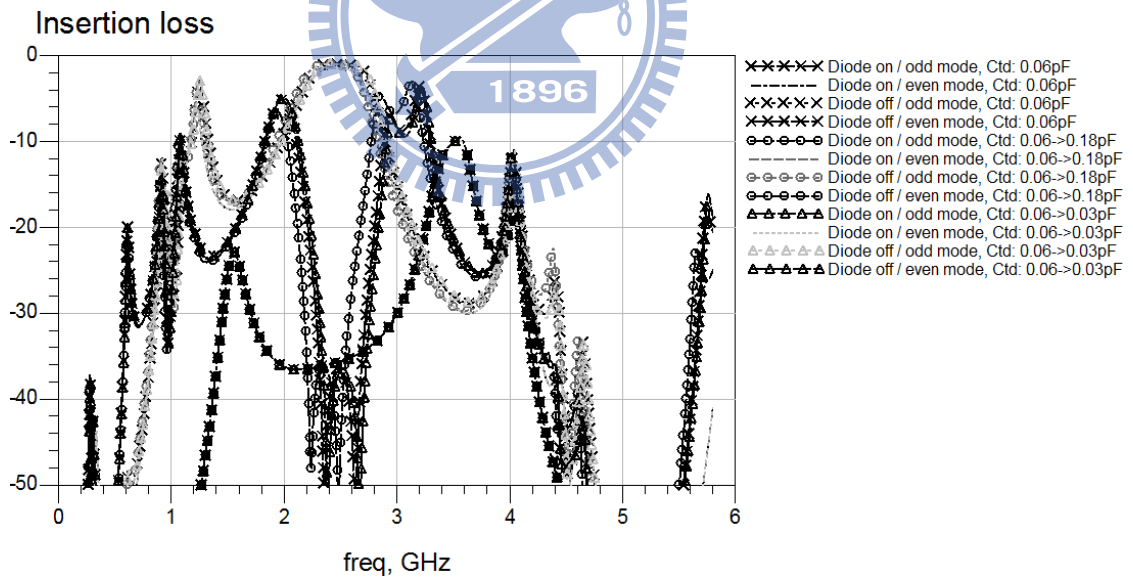


Figure 2.21 3D EM simulated insertion loss when diode capacitance changes

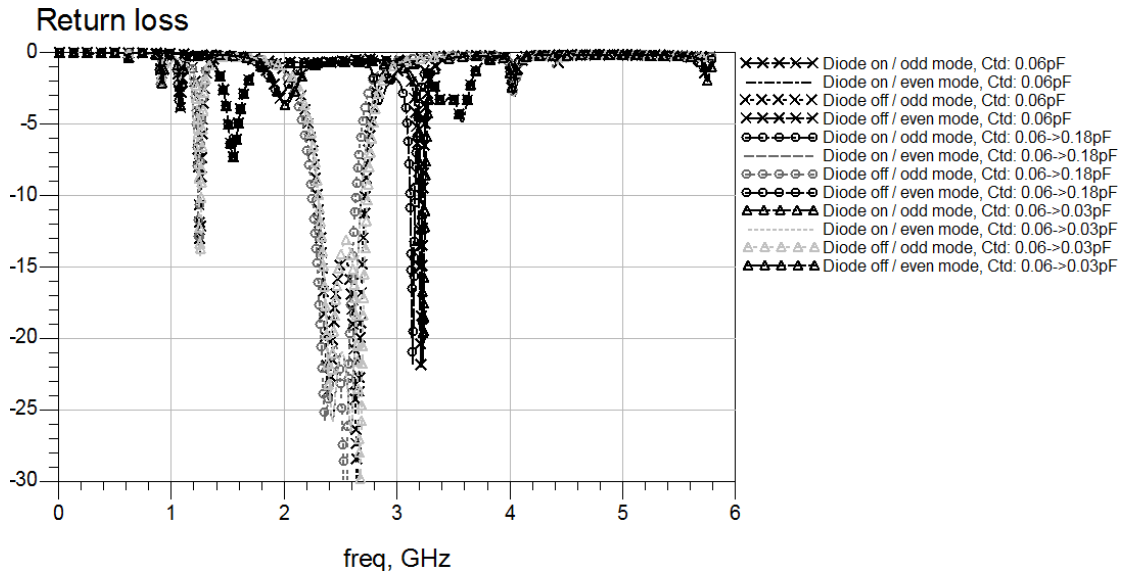


Figure 2.22 3D EM simulated return loss when diode capacitance changes

If the inductance of the diodes is changed from 0.4nH to 0.6nH or to 0.2nH, there will also be a frequency shift, and the insertion loss performance under diode on/odd mode will be changed as well. The bandwidth (pass-band insertion loss <3dB, stop-band insertion loss >31.438dB, pass-band return loss >14.290dB, stop-band return loss <3dB) will be decreased to 2.350GHz~2.637GHz.

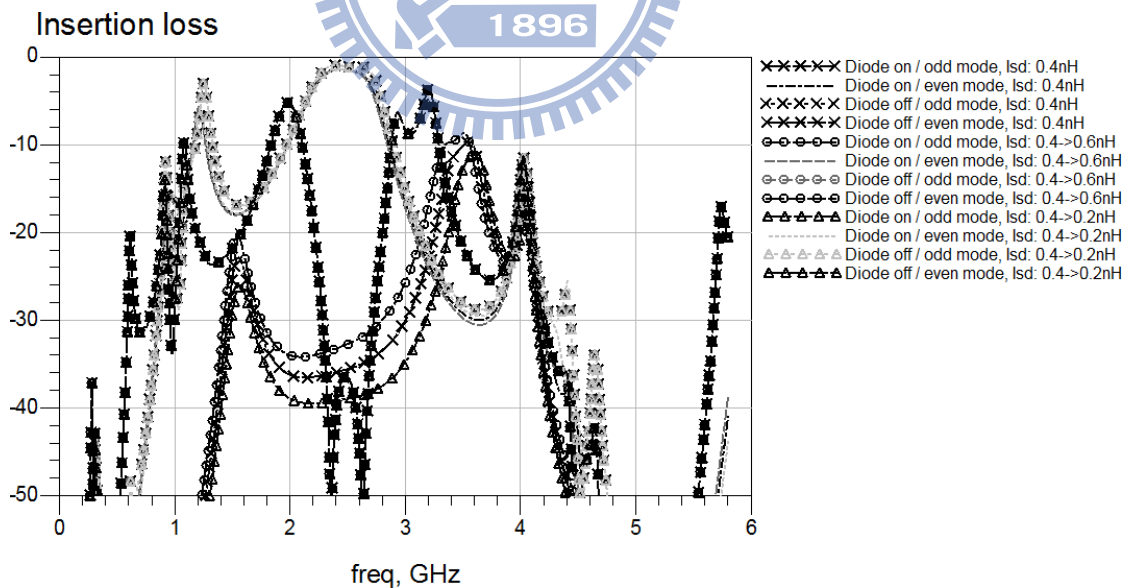


Figure 2.23 3D EM simulated insertion loss when diode inductance changes



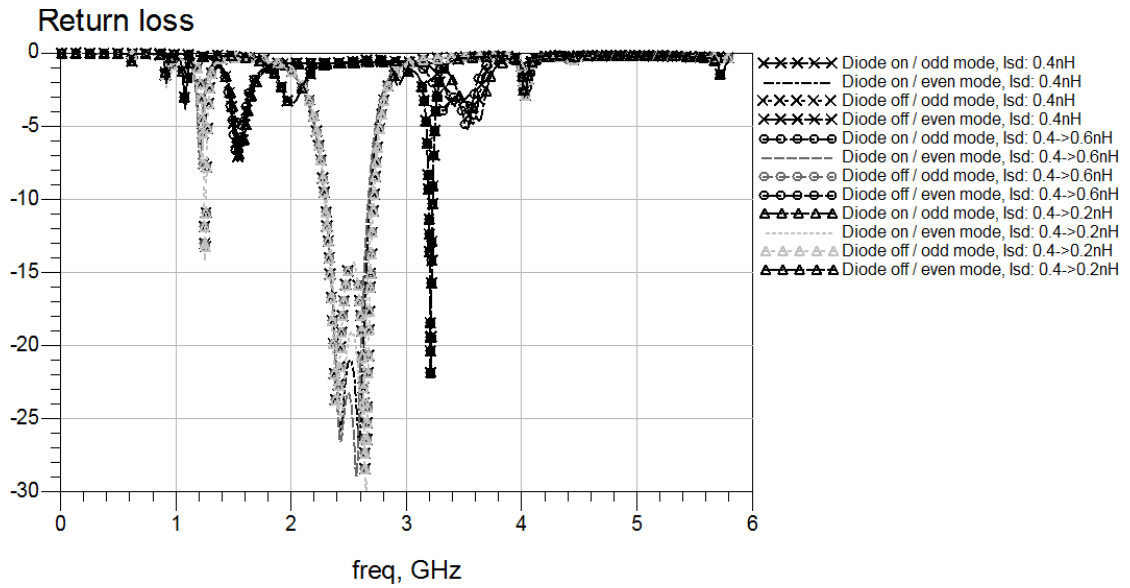


Figure 2.24 3D EM simulated return loss when diode inductance changes

If the resistance, capacitance, and inductance of the diodes are changed at the same time, the bandwidth (pass-band insertion loss <3dB, stop-band insertion loss >32.371dB, pass-band return loss >12.979dB, stop-band return loss <3dB) will be decreased to 2.340GHz~2.557GHz.

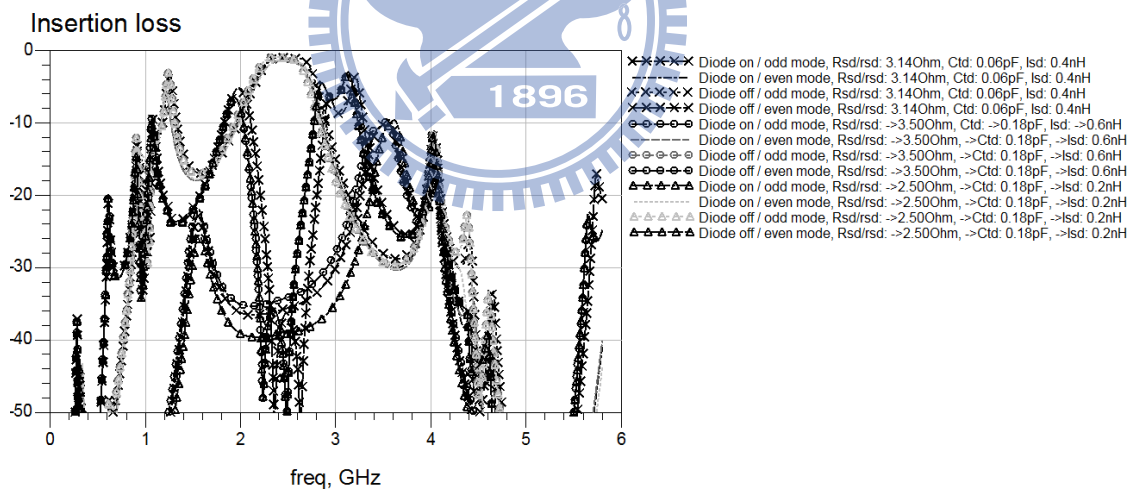


Figure 2.25 3D EM simulated insertion loss when diode resistance, capacitance, and inductance change

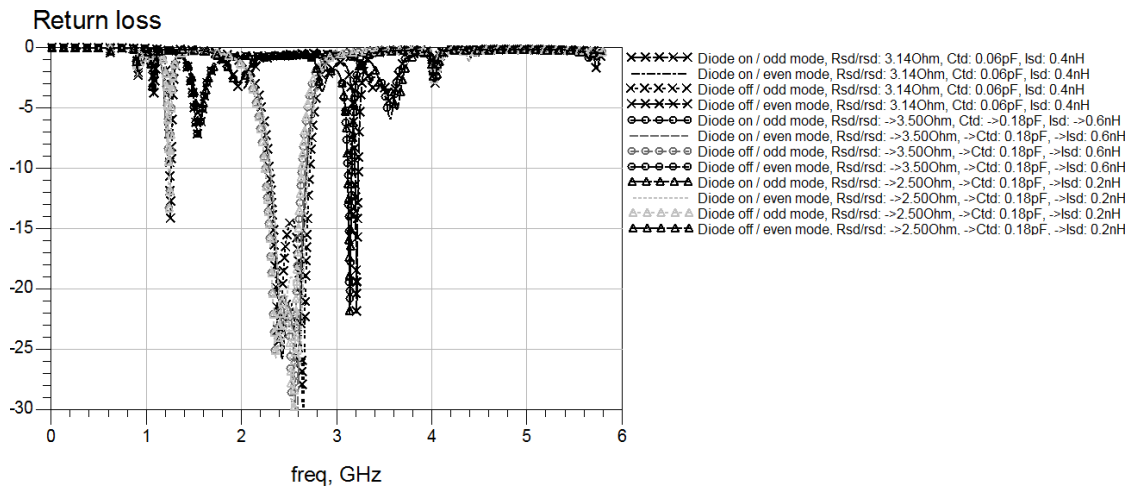
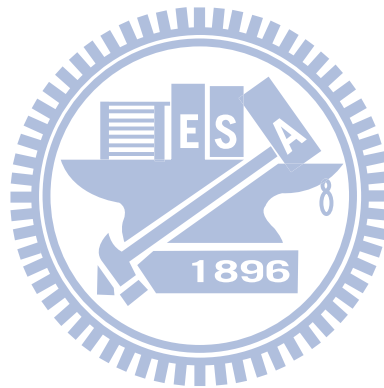


Figure 2.26 3D EM simulated return loss when diode resistance, capacitance, and inductance change



## Chapter 3 Microwave Filter Theorem

### 3.1 Reflection Coefficient and Input Impedance

Assume that the incident wave at  $z=0$  is  $V_0^+$ , and the reflected wave at  $z=0$  is  $V_0^-$ , and the source is at  $z=-l$ . Let the characteristic impedance  $Z_0$ , and the load impedance at the end of the transmission line  $Z_L \neq Z_0$ . The voltage along the ideal transmission line can be expressed as (1)[1][2]

$$V(z) = V_0^+ e^{-j\beta z} + V_0^- e^{j\beta z} \quad (1)$$

The current along the ideal transmission line can be expressed as (2)

$$I(z) = \frac{V_0^+}{Z_0} e^{-j\beta z} - \frac{V_0^-}{Z_0} e^{j\beta z} \quad (2)$$

At  $z=0$ , the relation between the voltage and the current is as (3)

$$Z_L = \frac{V_0}{I_0} = \frac{V_0^+ + V_0^-}{V_0^+ - V_0^-} \quad (3)$$

Rewrite equation (3), we can get  $V_0^-$

$$V_0^- = \frac{Z_L - Z_0}{Z_L + Z_0} V_0^+ \quad (4)$$

The ratio of the reflected voltage wave and the incident voltage wave is defined as the reflection coefficient  $\Gamma$

$$\Gamma = \frac{V_0^-}{V_0^+} = \frac{Z_L - Z_0}{Z_L + Z_0} \quad (5)$$

Figure 3.1 shows an ideal transmission line with length  $l$  and the load impedance  $Z_L$ .

The input impedance  $Z_{in} = Z_0 \frac{Z_L + jZ_0 \tan \beta l}{Z_0 + jZ_L \tan \beta l}$ .

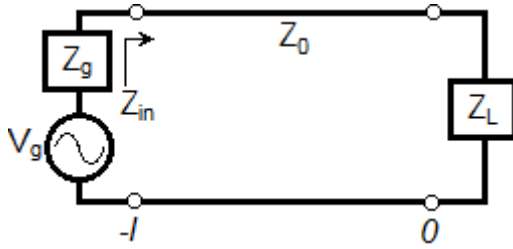


Figure 3.1 Transmission line circuit for mismatched load and generator

If the length  $l = \lambda/4$ ,  $\tan \beta l = \tan(\pi/2) = \infty$ , we can get  $Z_{in} = \frac{Z_0^2}{Z_L}$

The input impedance is 0 if the load is open circuit,  $Z_{in} = \frac{Z_0^2}{\infty} = 0$

The load impedance is  $\infty$  if the load is the short circuit,  $Z_{in} = \frac{Z_0^2}{0} = \infty$

### 3.2 S-Parameters

In microwave circuits analysis, it is too complicated if we use Maxwell equation to solve all the circuits. What we want to know is usually the voltage, current, or power at some point of the microwave circuits instead of the electrical field and magnetic field of that point. Therefore, we may simplify the circuits. For example, we may take the transmission line as many discrete components, and we may make use of network theorem or transmission theorem to analyze it.[3]

If the voltage and current are defined at all nodes within the network, we may use the matrix to describe the characteristics of the network.

In figure 3.2, the voltage and current of each  $t_n$  plane are

$$V_n = V_n^+ + V_n^- \quad (6)$$

$$I_n = I_n^+ - I_n^- \quad (7)$$

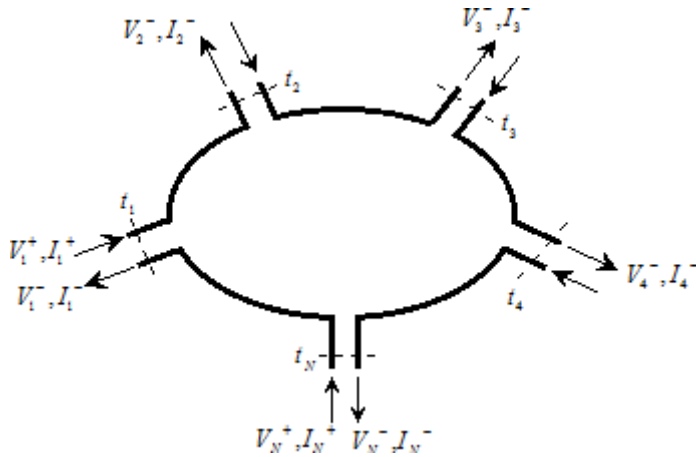


Figure 3.2 An arbitrary N-port microwave network

The impedance matrix, the relation between the voltage and the current is

$$\begin{bmatrix} V_1 \\ V_2 \\ \vdots \\ V_N \end{bmatrix} = \begin{bmatrix} Z_{11} & Z_{12} & \cdots & Z_{1N} \\ Z_{21} & & & \vdots \\ \vdots & & & \vdots \\ Z_{N1} & \cdots & \cdots & Z_{NN} \end{bmatrix} \begin{bmatrix} I_1 \\ I_2 \\ \vdots \\ I_N \end{bmatrix} \quad (8)$$

$$[V] = [Z][I] \quad (9)$$

The conductance matrix can be defined as below

$$\begin{bmatrix} I_1 \\ I_2 \\ \vdots \\ I_N \end{bmatrix} = \begin{bmatrix} Y_{11} & Y_{12} & \cdots & Y_{1N} \\ Y_{21} & & & \vdots \\ \vdots & & & \vdots \\ Y_{N1} & \cdots & \cdots & Y_{NN} \end{bmatrix} \begin{bmatrix} V_1 \\ V_2 \\ \vdots \\ V_N \end{bmatrix} \quad (10)$$

$$[I] = [Y][V] \quad (11)$$

A practical problem exists when trying to measure the voltages and currents at microwave frequencies. The scattering matrix relates the voltage waves incident on the ports to those reflected from the ports. For some circuits, the scattering parameters can be measured directly with a vector network analyzer. The scattering matrix is defined in relation to these incident and reflected voltage waves as

$$\begin{bmatrix} V_1^- \\ V_2^- \\ \vdots \\ V_N^- \end{bmatrix} = \begin{bmatrix} S_{11} & S_{12} & \cdots & S_{1N} \\ S_{21} & & & \vdots \\ \vdots & & & \vdots \\ S_{N1} & \cdots & \cdots & S_{NN} \end{bmatrix} \begin{bmatrix} V_1^+ \\ V_2^+ \\ \vdots \\ V_N^+ \end{bmatrix} \quad (12)$$

$$[V^-] = [S][V^+] \quad (13)$$

If the characteristic impedance  $Z_{0n}$  is the same for all ports (it is not required for generalized scattering coefficients), take  $Z_{0n} = 1$  for example, the voltage and current of port n are as below

$$V_n = V_n^+ + V_n^- \quad (14)$$

$$I_n = I_n^+ - I_n^- = V_n^+ - V_n^- \quad (15)$$

$$[Z][I] = [Z][V^+] - [Z][V^-] = [V] = [V^+] + [V^-] \quad (16)$$

$$([Z] + [U])[V^-] = ([Z] - [U])[V^+] \quad (17)$$

$$[S] = ([Z] + [U])^{-1}([Z] - [U]) \quad (18)$$

If it is a one port network, equation (18) can be simplified as below

$$S_{11} = \frac{z_{11} - 1}{z_{11} + 1} \quad (19)$$

The result is the same as the reflection coefficient when the normalized impedance of the load is  $z_{11}$ .

For some multi-port network whose characteristic impedance of each port is not the same, we may need to use generalized scattering matrix.

$$a_n = \frac{V_n^+}{\sqrt{Z_{0n}}} \quad (20)$$

$$b_n = \frac{V_n^-}{\sqrt{Z_{0n}}} \quad (21)$$

$$V_n = V_n^+ + V_n^- = \sqrt{Z_{0n}}(a_n + b_n) \quad (22)$$

$$I_n = I_n^+ - I_n^- = \frac{1}{\sqrt{Z_{0n}}} (a_n - b_n) \quad (23)$$

$$[b] = [S][a] \quad (24)$$

$$S_{ij} = \left. \frac{V_i^- \sqrt{Z_{0j}}}{V_j^+ \sqrt{Z_{0i}}} \right|_{V_k^+ = 0, k \neq j} \quad (25)$$

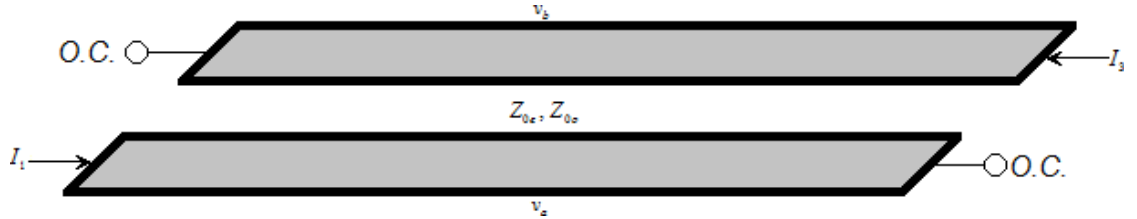


Figure 3.3 A two-port coupled line filter section

A parallel coupled line section is shown in figure 3.3, with port voltage and current definitions. By superposition, we see that the total port currents,  $I_i$ , can be expressed in terms of the even- and odd-mode currents as

$$I_1 = i_{1e} + i_{1o} \quad (26)$$

$$I_3 = i_{3e} + i_{3o} \quad (27)$$

First consider the line as being driven in the even mode by the  $i_{1e}$  current source. If the other ports are open-circuited, the input impedance at port 1 is

$$Z_{in}^e = -jZ_{0e} \cot \beta l \quad (28)$$

The voltage on the conductor can be expressed as

$$v_a^{1e}(z) = v_b^{1e}(z) = V_e^+ [e^{-j\beta(z-l)} + e^{j\beta(z-l)}] = 2V_e^+ \cos \beta(l-z) \quad (29)$$

$$v_a^{1e}(0) = v_b^{1e}(0) = 2V_e^+ \cos \beta l = i_{1e} Z_{in}^e \quad (30)$$

$$v_a^{1e}(z) = v_b^{1e}(z) = -jZ_{0e} \frac{\cos \beta(l-z)}{\sin \beta l} i_{1e} \quad (31)$$

Similarly, the voltages due to current source  $i_{3e}$  driving the line in the even mode are

$$v_a^{3e}(z) = v_b^{3e}(z) = -jZ_{0e} \frac{\cos \beta z}{\sin \beta l} i_{3e} \quad (32)$$

Now consider the line as being driven in the odd mode by current  $i_{1o}$ . If the other ports are open-circuited, the input impedance at port 1 is

$$Z_{in}^o = -jZ_{0o} \cot \beta l \quad (33)$$

The voltage on the conductor can be expressed as

$$v_a^{1o}(z) = -v_b^{1o}(z) = V_0^+ [e^{-j\beta(z-l)} + e^{j\beta(z-l)}] = 2V_0^+ \cos \beta(l-z) \quad (34)$$

Then the voltage at port 1 is

$$v_a^{1o}(0) = 2V_0^+ \cos \beta l = i_{1o} Z_{in}^o \quad (35)$$

$$v_a^{1o}(z) = -v_b^{1o}(z) = -jZ_{0o} \frac{\cos \beta(l-z)}{\sin \beta l} i_{1o} \quad (36)$$

Similarly, the voltages due to current  $i_{3o}$  driving the line in the odd mode are

$$v_a^{3o}(z) = -v_b^{3o}(z) = jZ_{0o} \frac{\cos \beta z}{\sin \beta l} i_{3o} \quad (37)$$

The total voltage at port 1 is

$$\begin{aligned} V_1 &= v_a^{1e}(0) + v_a^{1o}(0) + v_a^{3e}(0) + v_a^{3o}(0) \\ &= -j(Z_{0e} i_{1e} + Z_{0o} i_{1o}) \cot \theta - j(Z_{0e} i_{3e} - Z_{0o} i_{3o}) \csc \theta \end{aligned} \quad (38)$$

Where  $\theta = \beta l$

From symmetry, all the other matrix elements can be found once the first row is known.

The Z matrix elements are then

$$Z_{11} = Z_{33} = -\frac{j}{2}(Z_{0e} + Z_{0o}) \cot \theta \quad (39)$$

$$Z_{13} = Z_{31} = -\frac{j}{2}(Z_{0e} - Z_{0o}) \csc \theta \quad (40)$$

In figure 3.3,  $I_2 = I_4 = 0$ . A two-port network matrix equation can be expressed as below

$$V_1 = Z_{11}I_1 + Z_{13}I_3 \quad (41)$$

$$V_3 = Z_{31}I_1 + Z_{33}I_3 \quad (42)$$

We can analyze the filter characteristics of this circuit by calculating the image impedance and the propagation constant. The image impedance in terms of the Z-parameters is



$$Z_i = \sqrt{Z_{11}^2 - \frac{Z_{11}Z_{13}^2}{Z_{33}}} = \frac{1}{2} \sqrt{(Z_{0e} - Z_{0o})^2 \csc^2 \theta - (Z_{0e} + Z_{0o})^2 \cot^2 \theta} \quad (43)$$

When the coupled line section is  $\lambda/4$  ( $\theta = \pi/2$ ) long, the image impedance reduces to

$$Z_i = \frac{1}{2}(Z_{0e} - Z_{0o}) \quad (44)$$

Which is real and positive, since  $Z_{0e} > Z_{0o}$ . But when  $\theta \rightarrow 0$  or  $\pi$ ,  $Z_i \rightarrow \pm j\infty$ , indicating a stop-band. In figure 3.3, the coupling line with port 2 and port 4 open-circuited can be taken as a band-pass filter, which can be used to block the DC voltage.

### 3.3 Equal Ripple Filter

The perfect filter would have zero insertion loss in the pass-band, infinite attenuation in the stop-band, and a linear phase response in the pass-band. However, such filters do not exist in practice, so compromises must be made. If a Chebyshev polynomial[4] is used to specify the insertion loss of an N-order low-pass filter as

$$P_{LR} = \frac{P_{inc}}{P_{load}} = 1 + k^2 T_N^2\left(\frac{\omega}{\omega_C}\right) \quad (45)$$

The pass-band response will have ripples of amplitude  $1 + k^2$ , since  $T_N(x)$  oscillates between  $\pm 1$  for  $|x| \leq 1$ ,  $k^2$  determines the pass-band ripple level.

For an equal ripple low-pass filter with a cutoff frequency  $\omega_C = 1$ , the power loss ratio is

$$P_{LR} = \frac{P_{inc}}{P_{load}} = 1 + k^2 T_N^2(\omega) \quad (46)$$

Since the Chebyshev polynomials have the property that

$$T_N(0) = \begin{cases} 0 & N : \text{odd}, \\ 1 & N : \text{even}, \end{cases} \quad (47)$$

It shows that the filter will have a unity power loss ratio at  $\omega=0$  for N odd, but a

power loss ratio of  $1+k^2$  at  $\omega=0$  for N even.

For the two-element equal ripple filter,  $T_2(x) = 2x^2 + 1$ ,

$$1+k^2(4\omega^4 - 4\omega^2 + 1) = 1 + \frac{1}{4R} \left[ (1-R)^2 + (R^2C^2 + L^2 - 2LCR^2)\omega^2 + L^2C^2R^2\omega^4 \right] \quad (48)$$

which can be solved for R, L, and C if the equal ripple level (as determined by  $k^2$ ) is known. Thus, at  $\omega=0$  we have that

$$k^2 = \frac{(1-R)^2}{4R} \quad (49)$$

$$R = 1 + 2k^2 \pm 2k\sqrt{1+k^2} \quad (\text{for N even}) \quad (50)$$

Equating coefficients of  $\omega^2$  and  $\omega^4$  yields the additional relations,

$$4k^2 = \frac{1}{4R} L^2 C^2 R^2 \quad (51)$$

$$-4k^2 = \frac{1}{4R} (R^2 C^2 + L^2 - 2LCR^2) \quad (52)$$

which can be used to find L and C. From equation (50), we find that R is not unity, so there will be an impedance mismatch if the load actually has a unity(normalized) impedance; this can be corrected with a quarter-wave transformer, or by using an additional filter element to make N odd. For odd N, it can be shown that R=1. (This is because there is a unity power loss ratio at  $\omega=0$  for N odd.)

### 3.4 Impedance and Frequency Scaling

In the prototype design, the source and the load resistances are unity (except for equal-ripple filters with even N, which have non-unity load resistance). A source resistance of  $R_0$  can be obtained by multiplying the impedances of the prototype design by  $R_0$ . If we primes denote impedance scaled quantities, we have the new filter component values given by

$$L' = R_0 L \quad (53)$$

$$C' = \frac{C}{R_0} \quad (54)$$

$$R'_S = R_0 \quad (55)$$

$$R'_L = R_0 R_L \quad (56)$$

where L, C, and R<sub>L</sub> are the component values for the original prototype.

To change the cutoff frequency of a low-pass filter from unity to  $\omega_c$  requires that we scale the frequency dependence of the filter by the factor  $\frac{1}{\omega_c}$ , which is accomplished by replacing  $\omega$  by  $\frac{\omega}{\omega_c}$ .

Then the new power loss ratio will be

$$P'_{LR}(\omega) = P_{LR}\left(\frac{\omega}{\omega_c}\right) \quad (57)$$

where  $\omega_c$  is the new cutoff frequency. Cutoff occurs when  $\omega = \omega_c$ .

The new element values are determined by applying the new substitution of  $\omega \leftarrow \frac{\omega}{\omega_c}$  to the series reactances,  $j\omega L_k$ , and shunt susceptances,  $j\omega C_k$ , of the prototype filter.

Thus,

$$jX_k = j\frac{\omega}{\omega_c}L_k = j\omega L'_k \quad (58)$$

$$jB_k = j\frac{\omega}{\omega_c}C_k = j\omega C'_k \quad (59)$$

which shows that the new element values are given by

$$L'_k = \frac{L_k}{\omega_c} \quad (60)$$

$$C'_k = \frac{C_k}{\omega_c} \quad (61)$$

When both impedance and frequency scaling are required, the new element values are given by

$$L'_k = \frac{R_0 L_k}{\omega_c} \quad (62)$$

$$C'_k = \frac{C_k}{R_0 \omega_c} \quad (63)$$

### 3.5 Band-pass and Band-stop Transformation

Low-pass prototype filter design can be transformed to have the band-pass or band-stop responses illustrated in figure 3.4.

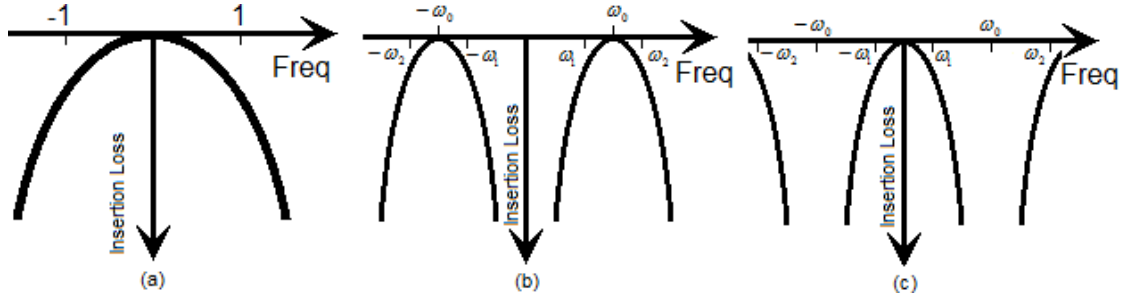


Figure 3.4 (a) Low-pass prototype (b) Transformation to band-pass filter (c) Transformation to band-stop filter

If  $\omega_1$  and  $\omega_2$  denote the edges of the pass-band, then a band-pass response can be obtained using the following frequency substitution:

$$\omega \leftarrow \frac{\omega_0}{\omega_2 - \omega_1} \left( \frac{\omega}{\omega_0} - \frac{\omega_0}{\omega} \right) = \frac{1}{\Delta} \left( \frac{\omega}{\omega_0} - \frac{\omega_0}{\omega} \right) \quad (64)$$

where  $\Delta = \frac{\omega_2 - \omega_1}{\omega_0}$  is the fractional bandwidth of the pass-band. If we choose  $\omega_0$  as

the geometric mean  $\omega_0 = \sqrt{\omega_1 \omega_2}$ , then the transformation maps the band-pass

characteristics of the figure 3.4(b) to the low-pass response of figure 3.4(a) as follows:

$$\frac{1}{\Delta} \left( \frac{\omega}{\omega_0} - \frac{\omega_0}{\omega} \right) = 0 \quad (65)$$

$$\frac{1}{\Delta} \left( \frac{\omega}{\omega_0} - \frac{\omega_0}{\omega} \right) = \frac{1}{\Delta} \left( \frac{\omega_1^2 - \omega_0^2}{\omega_0 \omega_1} \right) = -1 \quad (66)$$

$$\frac{1}{\Delta} \left( \frac{\omega}{\omega_0} - \frac{\omega_0}{\omega} \right) = \frac{1}{\Delta} \left( \frac{\omega_2^2 - \omega_0^2}{\omega_0 \omega_2} \right) = 1 \quad (67)$$

The new filter elements are determined as below:

$$jX_k = \frac{j}{\Delta} \left( \frac{\omega}{\omega_0} - \frac{\omega_0}{\omega} \right) L_k = j \frac{\omega L_k}{\Delta \omega_0} - j \frac{\omega_0 L_k}{\Delta \omega} = j\omega L'_k - j \frac{1}{\omega C'_k} \quad (68)$$

which shows that a series inductor  $L_k$  is transformed to a series LC circuit with element values,

$$L'_k = \frac{L_k}{\Delta \omega_0} \quad (69)$$

$$C'_k = \frac{\Delta}{\omega_0 L_k} \quad (70)$$

$$jB_k = \frac{j}{\Delta} \left( \frac{\omega}{\omega_0} - \frac{\omega_0}{\omega} \right) C_k = j \frac{\omega C_k}{\Delta \omega_0} - j \frac{\omega_0 C_k}{\Delta \omega} = j\omega C'_k - j \frac{1}{\omega L'_k} \quad (71)$$

which shows that a shunt capacitor  $C_k$  is transformed to a shunt LC circuit with element values,

$$L'_k = \frac{\Delta}{\omega_0 C_k} \quad (72)$$

$$C'_k = \frac{C_k}{\Delta \omega_0} \quad (73)$$

The inverse transformation can be used to obtain a band-stop response.

$$\omega \leftarrow \Delta \left( \frac{\omega}{\omega_0} - \frac{\omega_0}{\omega} \right)^{-1} \quad (74)$$

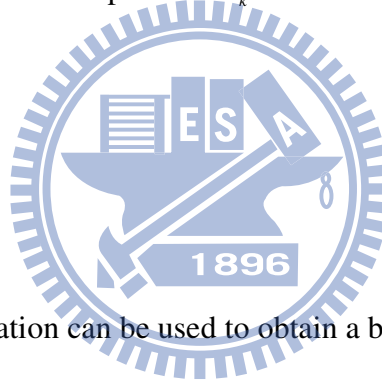
Then series inductors of the low-pass prototype are converted to parallel LC circuits with element values

$$L'_k = \frac{\Delta L_k}{\omega_0} \quad (75)$$

$$C'_k = \frac{1}{\omega_0 \Delta L_k} \quad (76)$$

The shunt capacitor of the low-pass prototype is converted to series LC with element values

$$L'_k = \frac{1}{\omega_0 \Delta C_k} \quad (77)$$



$$C'_k = \frac{\Delta C_k}{\omega_0} \quad (78)$$

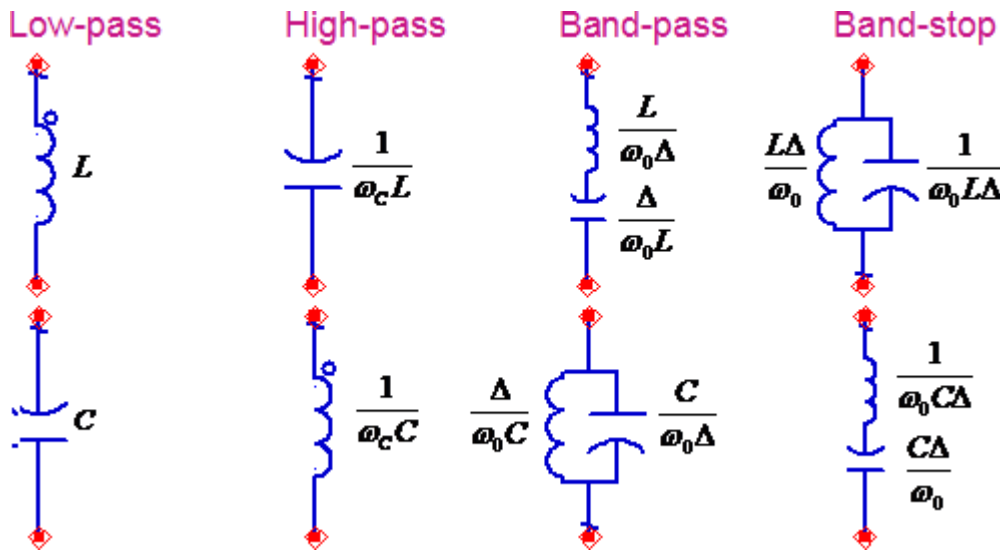


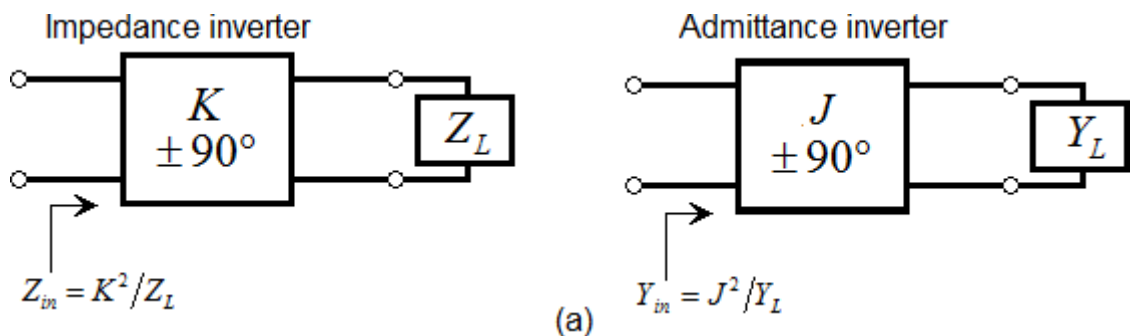
Figure 3.5 Summary of prototype filter transformation

### 3.6 Impedance and Admittance Inverters

It is often to use only series, or only shunt elements when implementing a filter with a particular type of transmission line. It is possible to use impedance or admittance inverters[5]. Such inverters are useful for implementing a band-pass or band-stop filter with narrow (<10%) bandwidth.

Since these inverters form the inverse of the load impedance or admittance, they can be used to transform series-connected elements to shunt-connected elements, or vice versa.

In its simplest form, a J or K inverter can be constructed using a quarter-wave transformer of the appropriate characteristic impedance, as shown in figure 3.6(b).



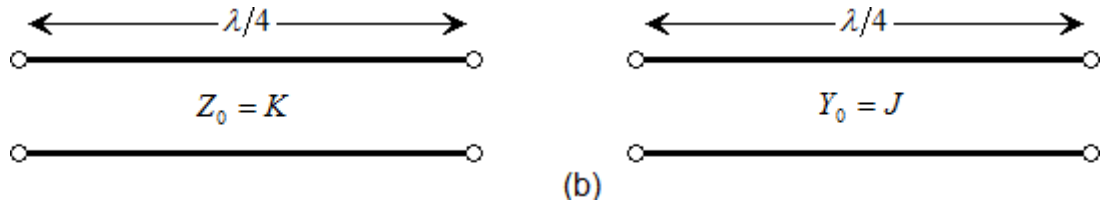
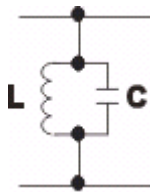


Figure 3.6 Impedance and admittance inverters (a)Operation of impedance and admittance inverters (b)Impedance as quarter-wave transformation

Series LC resonators and parallel LC resonators are used in band-pass and band-stop prototype filter. The resonance frequency  $\omega_0 = \frac{1}{\sqrt{LC}}$  of the resonator is not enough to

describe the characteristics of the resonator. We define the susceptance slope parameter

$$b_j = \frac{\omega_0}{2} \frac{dB_j(\omega)}{d\omega} \Big|_{\omega=\omega_0} = \omega_0 C_j = \frac{1}{\omega_0 L_j} \quad (79)$$



As for the series LC resonator, we define the reactance slope parameter

$$x_k = \frac{\omega_0}{2} \frac{dX_k(\omega)}{d\omega} \Big|_{\omega=\omega_0} = \omega_0 L_k = \frac{1}{\omega_0 C_k} \quad (80)$$

We may convert a parallel component  $Y_p$  to a series component  $Z_s$  via J converter, or we may convert a series component  $Z_s$  to a parallel component  $Y_p$  via K converter.

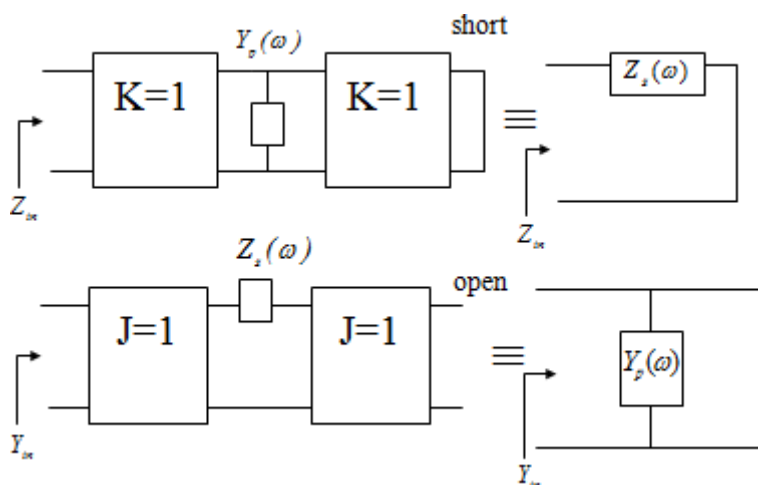


Figure 3.7 Impedance and admittance inverters

$$Z_{in} = \frac{K^2}{Z_p} = K^2 Y_p = Y_p = Z_s \quad (K = 1) \quad (81)$$

If  $Y_p$  is a parallel resonator,  $Y_p = j\omega C - \frac{j}{\omega L} = j\omega C \left(1 - \frac{\omega_0^2}{\omega^2}\right)$ , where  $\omega_0^2 = \frac{1}{LC}$ . If

$Z_s$  is a series resonator,  $Z_s = j\omega L - \frac{j}{\omega C} = j\omega L \left(1 - \frac{\omega_0^2}{\omega^2}\right)$ , where  $\omega_0^2 = \frac{1}{LC}$ .

From equation (81), we may get  $L=C$ . If we would like to change the relation between  $L$  and  $C$ , then  $K$  will be changed as well.

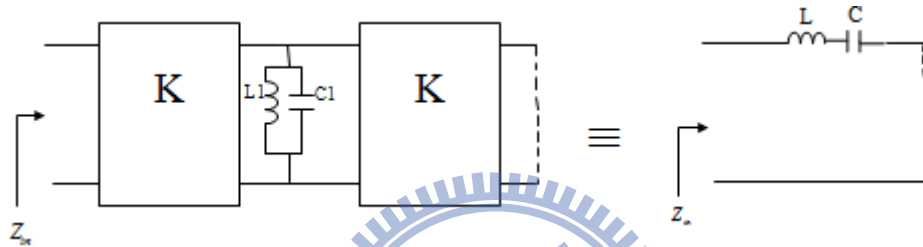


Figure 3.8 Impedance inverter

$$Z_{in} = K^2 \cdot (Y_p) = K^2 \left[ j\omega C_1 \left(1 - \frac{\omega_0^2}{\omega^2}\right) \right] \quad (82)$$

$$Z_{in} = j\omega L \left(1 - \frac{\omega_0^2}{\omega^2}\right) \quad (83)$$

Compare the equation (82) and (83), we may get

$$K = \sqrt{\frac{L}{C_1}} \quad (84)$$

The analysis of J converter is similar to that of K converter. We may get

$$Y_{in} = \frac{J^2}{Y_s} = J^2 Z_s = Y_p \quad (J = 1) \quad (85)$$

If we would like to change the relation between  $L$  and  $C$ , then  $J$  will be changed as well.

$$J = \sqrt{\frac{C}{L_1}} \quad (86)$$

We can make use of this feature to convert the filter to all series circuits or all shunt



circuits. From below figure, we may easily change the component value of the series resonators or the parallel resonators.

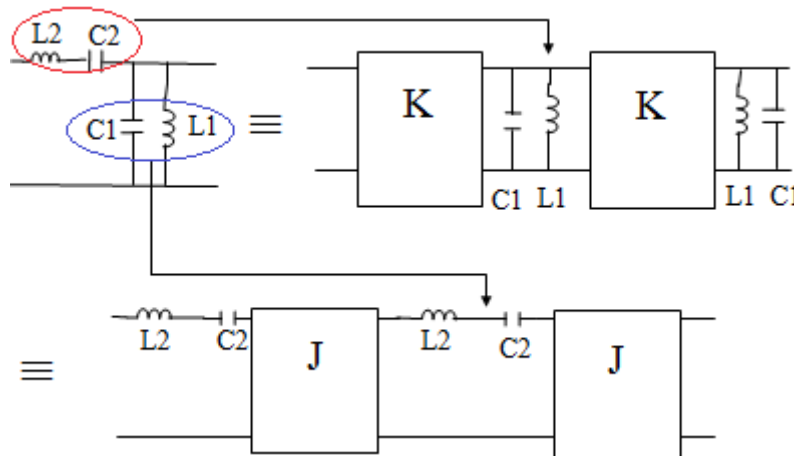


Figure 3.9 Impedance and admittance inverters

$$Z_{in} = K^2 \left[ j\omega C_1 \left( 1 - \frac{\omega_0^2}{\omega^2} \right) \right] = j\omega L_2 \left( 1 + \frac{\omega_0^2}{\omega^2} \right) \quad (87)$$

$$K = \sqrt{\frac{L_2}{C_1}} \quad (88)$$

$$Y_{in} = J^2 \left[ j\omega L_2 \left( 1 - \frac{\omega_0^2}{\omega^2} \right) \right] = j\omega C_1 \left( 1 + \frac{\omega_0^2}{\omega^2} \right) \quad (89)$$

$$J = \sqrt{\frac{C_1}{L_2}} \quad (90)$$

$$Y = j\omega C \left( 1 - \frac{\omega_0^2}{\omega^2} \right) = j\omega_0 C \left( \frac{\omega}{\omega_0} - \frac{\omega_0}{\omega} \right) = j b \cdot \left( \frac{\omega}{\omega_0} - \frac{\omega_0}{\omega} \right) \quad (91)$$

$$Z = j\omega L \left( 1 - \frac{\omega_0^2}{\omega^2} \right) = j\omega_0 L \left( \frac{\omega}{\omega_0} - \frac{\omega_0}{\omega} \right) = j x \cdot \left( \frac{\omega}{\omega_0} - \frac{\omega_0}{\omega} \right) \quad (92)$$

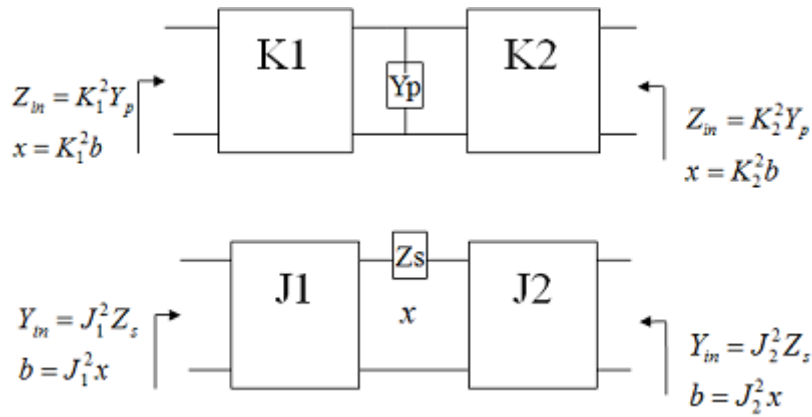


Figure 3.10 Impedance and admittance inverters

The slope parameter will be changed once K or J is changed. Since the left circuit and the right circuit are equivalent in the below figure, the susceptance of the two circuits will be equivalent. We can get

$$\frac{x_1}{K'^2} = \frac{x_0}{K^2} \quad (93)$$

$$K = K' \cdot \sqrt{\frac{x_0}{x_1}} = K' \cdot \sqrt{\frac{L_0}{L_1}} \quad (94)$$

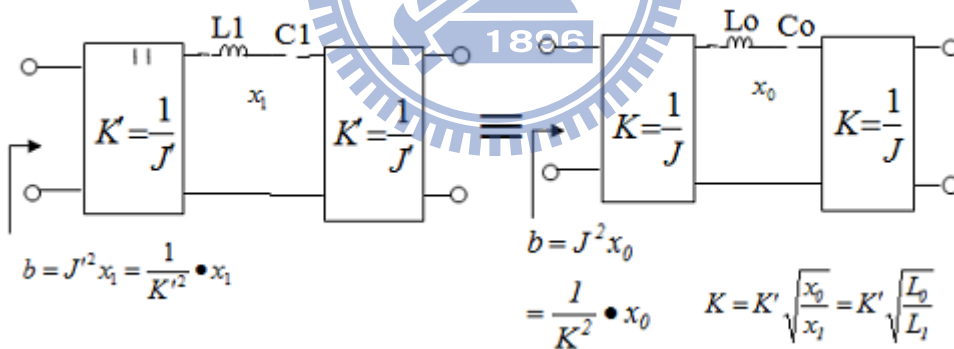


Figure 3.11 Impedance scaling of the K inverter

Similarly, the reactance of the left circuit and the right circuit in the below figure are equivalent.

$$\frac{b_1}{J'^2} = \frac{b_0}{J^2} \quad (95)$$

$$J = J' \cdot \sqrt{\frac{b_0}{b_1}} = J' \cdot \sqrt{\frac{C_0}{C_1}} \quad (96)$$

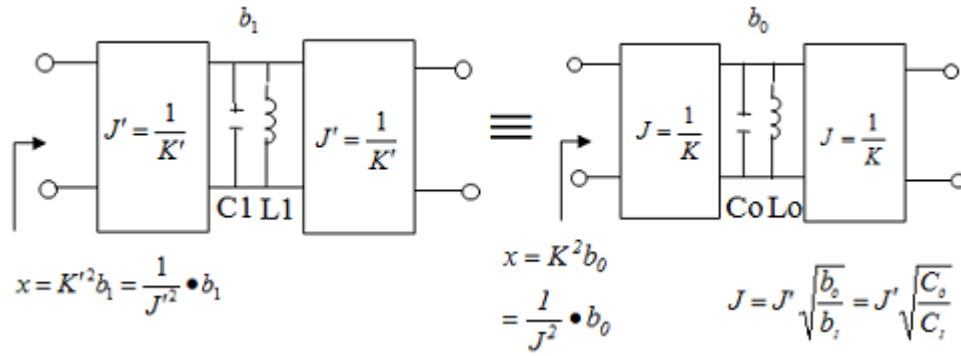


Figure 3.12 Admittance scaling of the J inverter

If the value of K in the left circuit is not the same as the value of K in the right circuit, we can still get the relationship in figure 3.13.

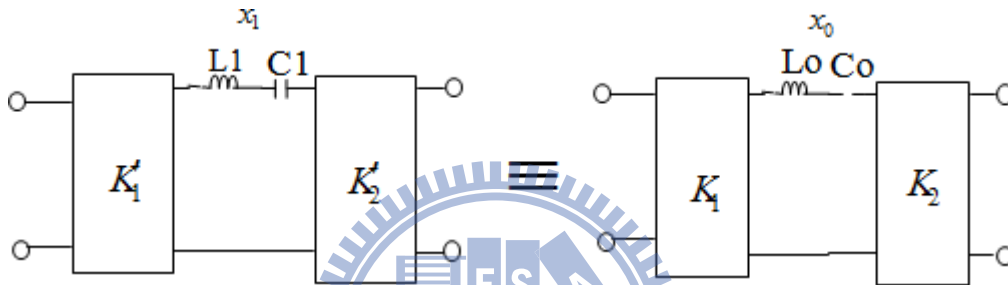


Figure 3.13 Impedance scaling of the K inverter

$$K_1 = K_1' \cdot \sqrt{\frac{x_0}{x_1}} = K_1' \cdot \sqrt{\frac{L_0}{L_1}} \quad (97)$$

$$K_2 = K_2' \cdot \sqrt{\frac{x_0}{x_1}} = K_2' \cdot \sqrt{\frac{L_0}{L_1}} \quad (98)$$

We can get similar relationship as below for J converter:

$$J_1 = J_1' \cdot \sqrt{\frac{b_0}{b_1}} = J_1' \cdot \sqrt{\frac{C_0}{C_1}} \quad (99)$$

$$J_2 = J_2' \cdot \sqrt{\frac{b_0}{b_1}} = J_2' \cdot \sqrt{\frac{C_0}{C_1}} \quad (100)$$

### 3.7 Band-stop and Band-pass Filters Using Quarter-Wave Resonators

The quarter-wave open-circuited or short-circuited transmission line stubs look like series or parallel resonant circuits, respectively. Thus we can use such stubs in shunt along a transmission line to implement band-pass or band-stop filters.

Quarter-wavelength sections of line between the stubs act as admittance inverters to effectively convert alternative shunt resonators to series resonators. The stub and the transmission line sections are  $\lambda/4$  long at the center frequency  $\omega_0$ .

For narrow bandwidths the response of such a filter using  $N$  stubs is essentially the same as that of a coupled line filter using  $N+1$  sections. The internal impedance of the stub filter is  $Z_0$ , while in the case of the coupled line filter end sections are required to transform the impedance level. This makes the stub filter more compact and easier to design.

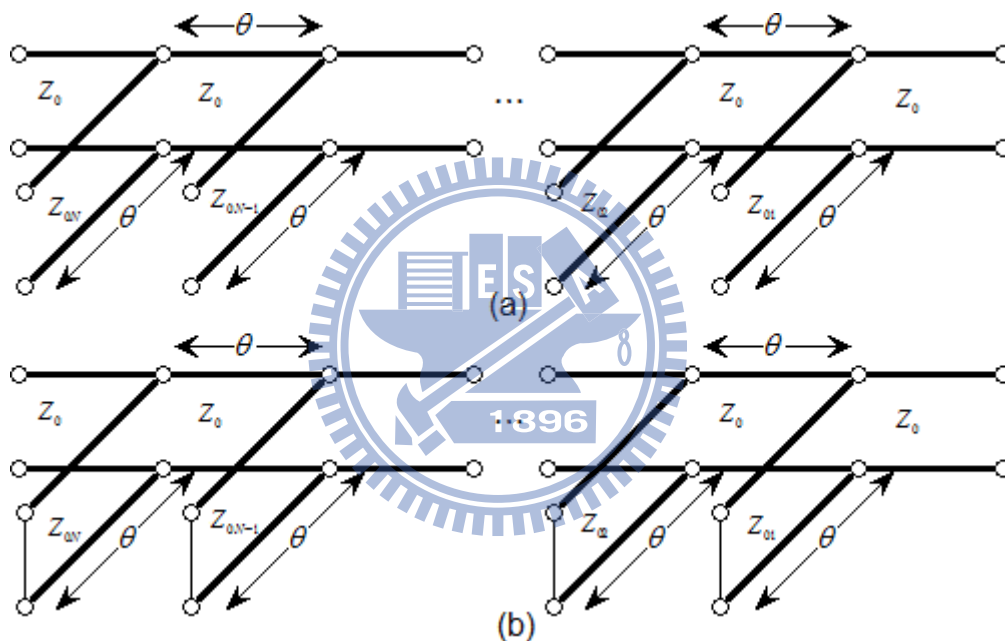


Figure 3.14 Band-stop and band-pass filters using shunt transmission line resonators ( $\theta = \pi/2$  at the center frequency) (a)Band-stop filter (b)Band-pass filter

Consider a band-stop filter using  $N$  open-circuited stubs, the design equations for the required stub characteristic impedances,  $Z_{0n}$ , will be derived in terms of the element values of a low-pass filter prototype through the use of the equivalent circuit. The analysis of band-pass filter using short-circuited stubs follows the same procedure.

An open-circuited stubs can be approximated as a series LC resonator when its length is near  $90^\circ$ . The input impedance of an open-circuited transmission line of characteristic impedance  $Z_{0n}$  is

$$Z = -jZ_{0n} \cot \theta \quad (101)$$

where  $\theta = \pi/2$  for  $\omega = \omega_0$ . If we let  $\omega = \omega_0 + \Delta\omega$ , where  $\Delta\omega \ll \omega_0$ , then  $\theta = \pi/2 \cdot (1 + \Delta\omega/\omega_0)$ , and this impedance can be approximated as

$$Z = jZ_{0n} \tan \frac{\pi\Delta\omega}{2\omega_0} \cong \frac{jZ_{0n}\pi(\omega - \omega_0)}{2\omega_0} \quad (102)$$

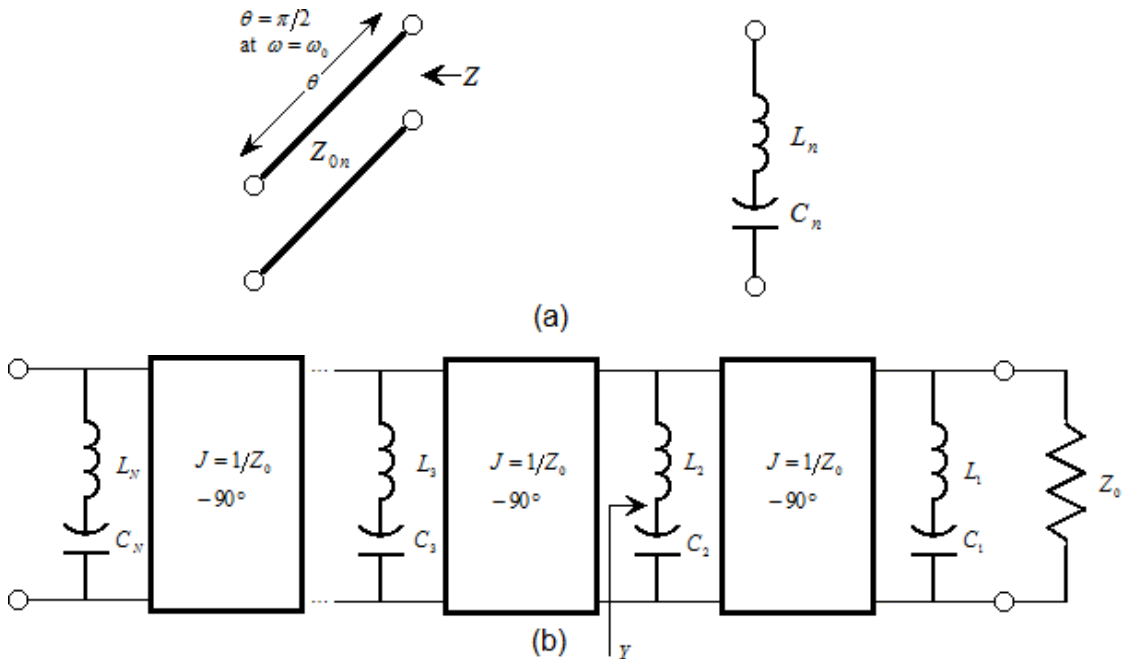
for frequency in the vicinity of the center frequency  $\omega_0$ . The impedance of a series LC circuit is

$$Z = j\omega L_n + \frac{1}{j\omega C_n} = j\sqrt{\frac{L_n}{C_n}} \left( \frac{\omega}{\omega_0} - \frac{\omega_0}{\omega} \right) \cong 2j\sqrt{\frac{L_n}{C_n}} \frac{\omega - \omega_0}{\omega_0} \cong 2jL_n(\omega - \omega_0) \quad (103)$$

where  $L_n C_n = 1/\omega_0^2$ . The characteristic impedance of the stub in terms of the resonator parameters:

$$Z_{0n} = \frac{4\omega_0 L_n}{\pi} \quad (104)$$

If we consider the quarter-wave sections of line between the stubs as ideal admittance inverters, the band-stop filter can be represented by the equivalent circuit of figure 3.15(b). The circuit elements of the equivalent circuit can be related to those of the lumped-element band-stop filter prototype of figure 3.15(c).



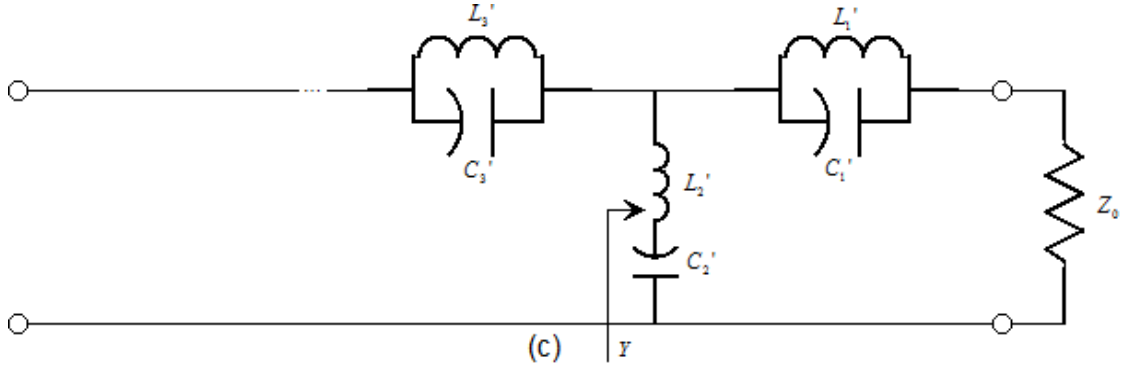


Figure 3.15 Equivalent circuit for the band-stop filter. (a)Equivalent circuit of open-circuited stub for  $\theta$  near  $\pi/2$  (b)Equivalent filter circuit using resonators and admittance inverter (c)Equivalent lumped-element band-stop filter

With reference to figure 3.15(b), the admittance,  $Y$ , seen looking toward the  $L_2C_2$  resonator is

$$Y = \frac{1}{j\omega L_2 + (1/j\omega C_2)} + \frac{1}{Z_0^2 \left[ \frac{1}{j\omega L_1 + (1/j\omega C_1)} + \frac{1}{Z_0} \right]^{-1}} \quad (105)$$

$$= \frac{1}{j\sqrt{L_2/C_2} [(\omega/\omega_0) - (\omega_0/\omega)]} + \frac{1}{Z_0^2 \left\{ \frac{1}{j\sqrt{L_1/C_1} [(\omega/\omega_0) - (\omega_0/\omega)]} + (1/Z_0) \right\}^{-1}}$$

The admittance at the corresponding point in the circuit of figure 3.15(c) is

$$Y = \frac{1}{j\omega L_2' + (1/j\omega C_2')} + \left[ \frac{1}{j\omega C_1' + (1/j\omega L_1')} + \frac{1}{Z_0} \right]^{-1} \quad (106)$$

$$= \frac{1}{j\sqrt{L_2'/C_2'} [(\omega/\omega_0) - (\omega_0/\omega)]} + \left\{ \frac{1}{j\sqrt{C_1'/L_1'} [(\omega/\omega_0) - (\omega_0/\omega)]} + Z_0 \right\}^{-1}$$

These two results will be equivalent if the following conditions are satisfied:

$$\frac{1}{Z_0^2} \sqrt{\frac{L_1}{C_1}} = \sqrt{\frac{C_1'}{L_1'}} \quad (107)$$

$$\sqrt{\frac{L_2}{C_2}} = \sqrt{\frac{L_2'}{C_2'}} \quad (108)$$

Since  $L_n C_n = L_n' C_n' = 1/\omega_0^2$ , these results can be solved for  $L_n$ :

$$L_1 = \frac{Z_0^2}{\omega_0^2 L_1'} \quad (109)$$

$$L_2 = L_2' \quad (110)$$

We can get

$$Z_{01} = \frac{4\omega_0 L_1}{\pi} = \frac{4Z_0^2}{\pi\omega_0 L'_1} = \frac{4Z_0}{\pi g_1 \Delta} \quad (111)$$

$$Z_{02} = \frac{4\omega_0 L_2}{\pi} = \frac{4\omega_0 L'_2}{\pi} = \frac{4Z_0}{\pi g_2 \Delta} \quad (112)$$

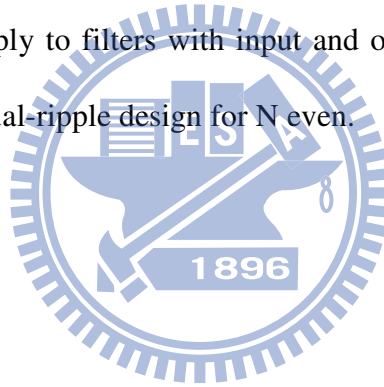
where  $\Delta = (\omega_2 - \omega_1)/\omega_0$  is the fractional bandwidth of the filter. The characteristic impedances of a band-stop filter is

$$Z_{0n} = \frac{4Z_0}{\pi g_n \Delta} \quad (113)$$

The characteristic impedances of a band-pass filter with short-circuited stub resonators is

$$Z_{0n} = \frac{\pi Z_0 \Delta}{4g_n} \quad (114)$$

These results only apply to filters with input and output impedances of  $Z_0$ , and so it cannot be used for equal-ripple design for N even.



## Chapter 4 Circuit Implementation

### 4.1 Chebyshev Low-pass Filter

We can get below parameters for Chebyshev low-pass prototype filter.

$$g_0 = 1 \quad (115)$$

$$R_L = 10 \cdot \log_{10} \left( 1 - 10^{-\frac{L_{ar}}{10}} \right) \quad (116)$$

$$\beta = \ln \left( \coth \frac{-L_{ar}}{17.37} \right) \quad (117)$$

$$\gamma = \sinh \left( \frac{\beta}{2N} \right) \quad (118)$$

$$a_k = \sin \left[ \frac{(2k-1)\pi}{2N} \right] \quad (119)$$

$$b_k = \gamma^2 + \sin^2 \left( \frac{k\pi}{N} \right) \quad (120)$$

$$g_0 = 1 \quad (121)$$

$$g_1 = \frac{2a_1}{\gamma} \quad (122)$$

$$g_k = \frac{4a_{k-1}a_k}{b_{k-1}g_{k-1}} \quad (123)$$

$$g_{N+1} = 1 \quad (\text{for odd } N) \quad (124)$$

$$g_{N+1} = \coth^2 \left( \frac{\beta}{4} \right) \quad (\text{for even } N) \quad (125)$$



### 4.2 Band-pass Filter

If we design  $R_L = -17$  (17dB return loss at the pass-band), we can get

$L_{ar} = -8.75 \times 10^{-2}$  (0.0875 dB ripple at the pass-band), and the value of g elements of

low-pass prototype filter are as below.

Table 4.1 The elements of low-pass prototype filter of return loss 17dB

$g_0$	$g_1$	$g_2$	$g_3$
1	0.8112	0.6104	1.3290

If we design  $f_0 = 2.5GHz$ ,  $\Delta = 0.15$ , we can get the lumped elements of the

band-pass filter as below.



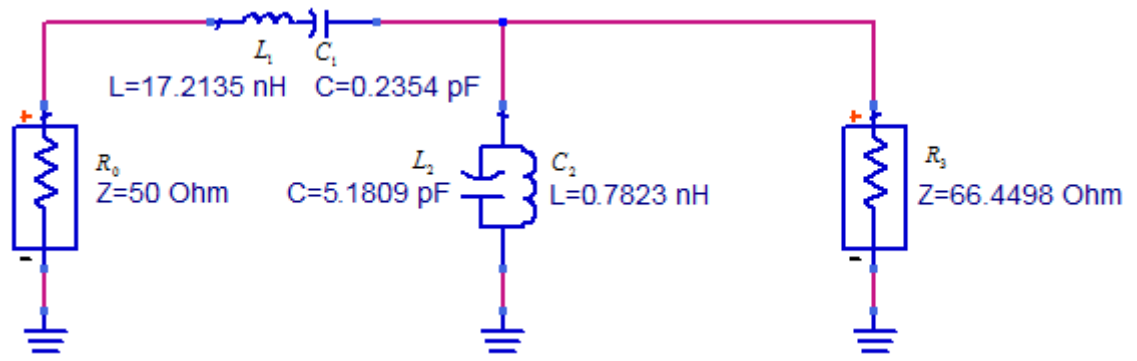


Figure 4.1 Band-pass filter of return loss 17dB, center frequency 2.5GHz, fractional bandwidth 15%

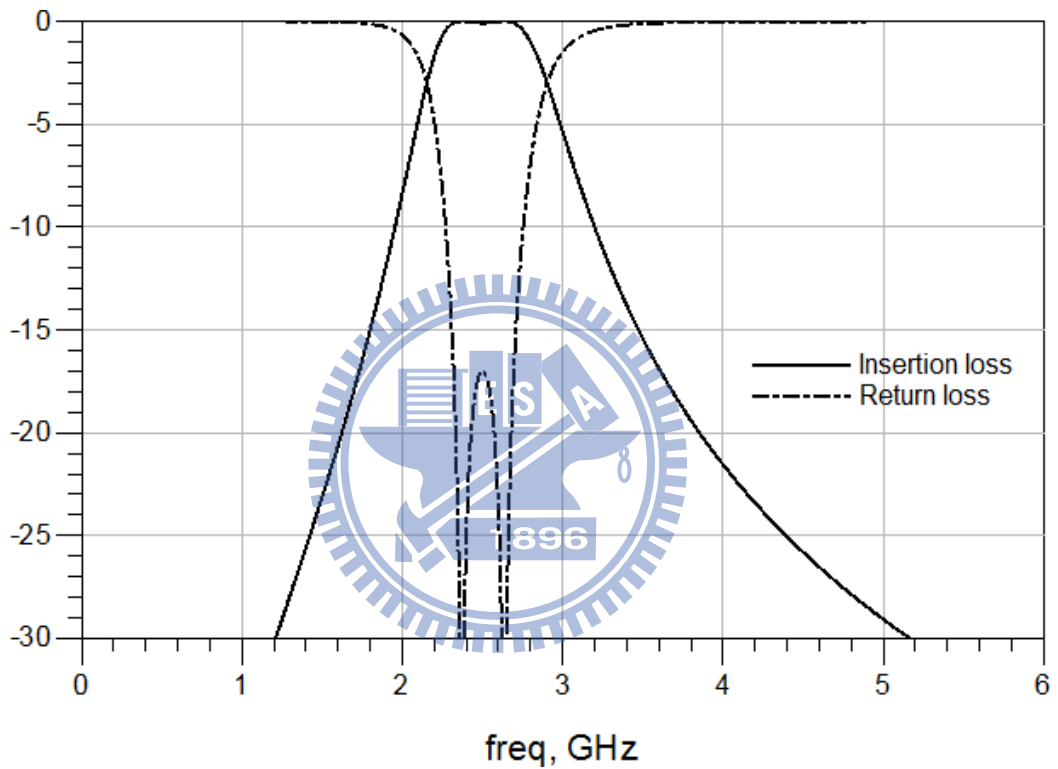


Figure 4.2 Simulated insertion loss and return loss of the band-pass filter in figure 4.1

We can make use of equation (88) to transfer the series LC into the inverters and shunt LC.

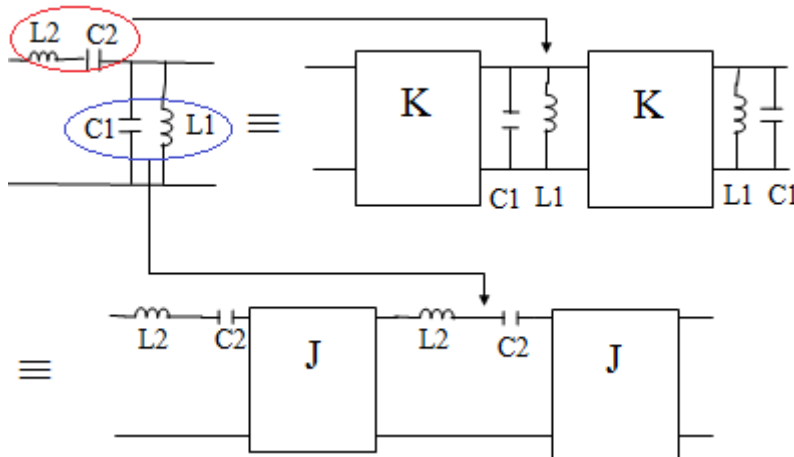


Figure 4.3 Impedance and admittance inverters

From equation (96), we can change the impedance of the J inverters. We can also change the load impedance to 50 Ohm.

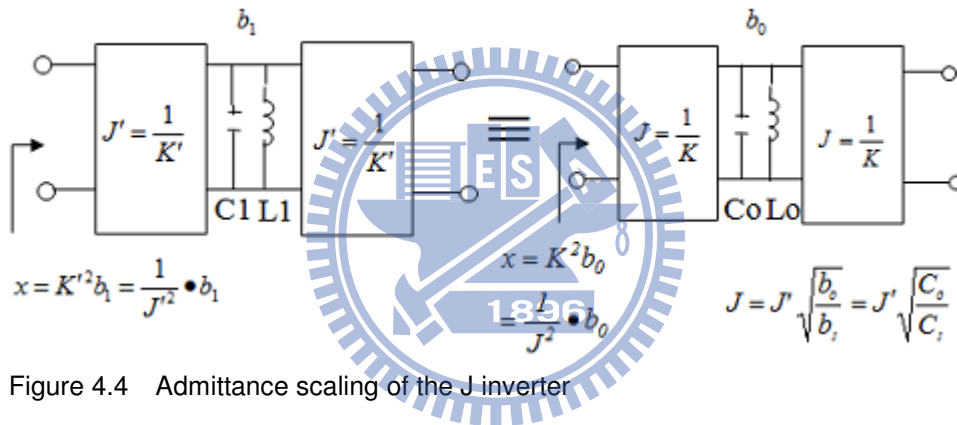


Figure 4.4 Admittance scaling of the J inverter

The equivalent circuit is as below.

Table 4.2 The elements of low-pass prototype filter of return loss 17dB

$R_L$	$Z_1$	$C_{pbb}$	$L_{pbb}$	$Z_2$
21.6191 Ohm	45.7788 Ohm	3.5515pF	1.1412nH	84.0868 Ohm

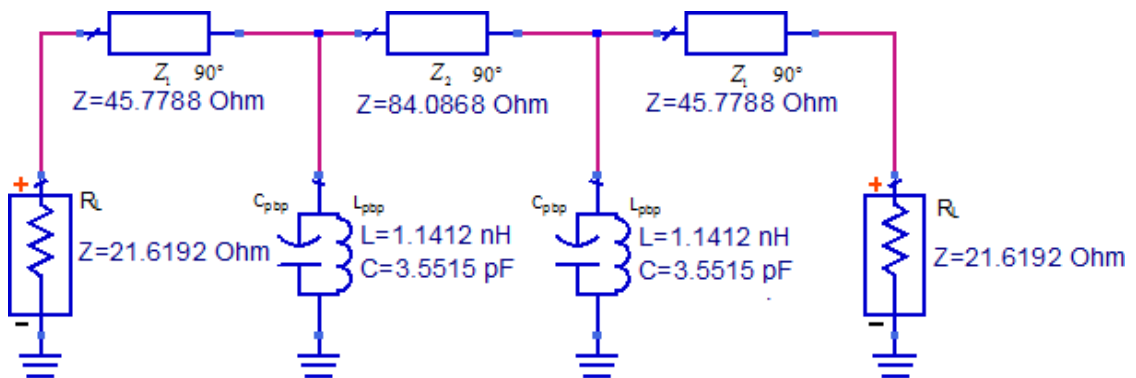


Figure 4.5 Band-pass filter of return loss 17dB, center frequency 2.5GHz, fractional bandwidth 15%

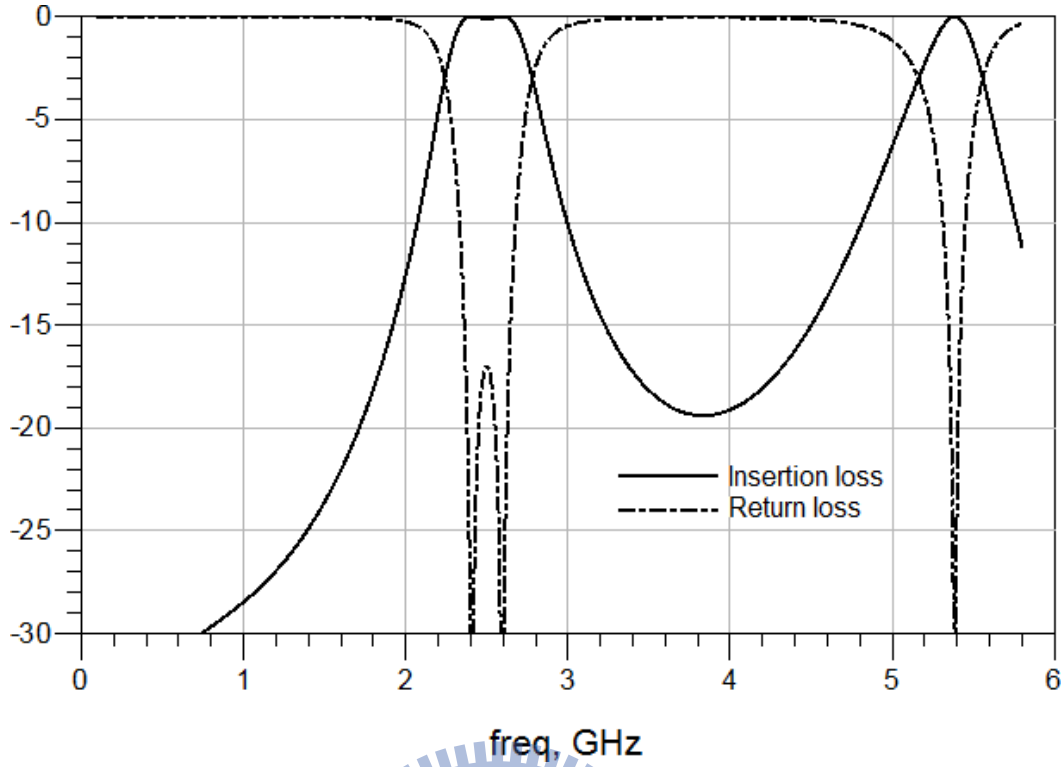


Figure 4.6 Simulated insertion loss and return loss of the band-pass filter in figure 4.5

From figure 3.3(c) and equation (44),  $\lambda/4$  coupled line can be taken as a transmission line of impedance  $Z_i = \frac{1}{2}(Z_{0e} - Z_{0o})$ . When we design the coupled line with line width  $w = 10\text{mil}$  and line spacing  $s = 8\text{mil}$ , we can get  $Z_{0e} = 130.686\Omega$  and  $Z_{0o} = 64.9301\Omega$ , and it can be taken as a transmission line of impedance  $Z_i = \frac{1}{2}(Z_{0e} - Z_{0o}) = 32.8780\Omega$  if the trace length is  $\lambda/4$  at the operation frequency. If the load impedance of the coupled line is 50 Ohm, the input impedance is

$$Z_{in} = \frac{Z_0^2}{Z_L} = \frac{32.8780^2}{50} = 21.6192\Omega.$$

We can use the equivalent short-circuited stub to implement the shunt LC resonator.

The input admittance of the short-circuited stub can be approximated as

$$Y = jY_0 \tan \frac{\pi\Delta\omega}{2\omega_0} \cong jY_0 \cdot \frac{\pi(\omega - \omega_0)}{2\omega_0} \quad (126)$$

The input admittance of the shunt LC resonator can be expressed as

$$Y = j\omega C + \frac{1}{j\omega L} = j\omega_0 C \left( \frac{\omega}{\omega_0} - \frac{\omega_0}{\omega} \right) \cong j\omega_0 C \cdot \frac{2(\omega - \omega_0)}{\omega_0} \quad (127)$$

We can get the characteristic impedance of the equivalent short-circuited stub by equation (126) and equation (127).

$$jY_0 \cdot \frac{\pi(\omega - \omega_0)}{2\omega_0} = j\omega_0 C \cdot \frac{2(\omega - \omega_0)}{\omega_0} \quad (128)$$

$$Z_0 = \frac{1}{Y_0} = \frac{\pi}{4\omega_0 C} \quad (129)$$

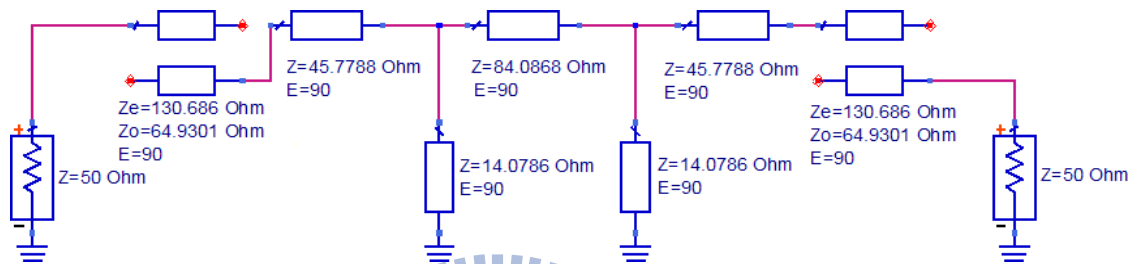


Figure 4.7 Band-pass filter of return loss 17dB, center frequency 2.5GHz, fractional bandwidth 15%

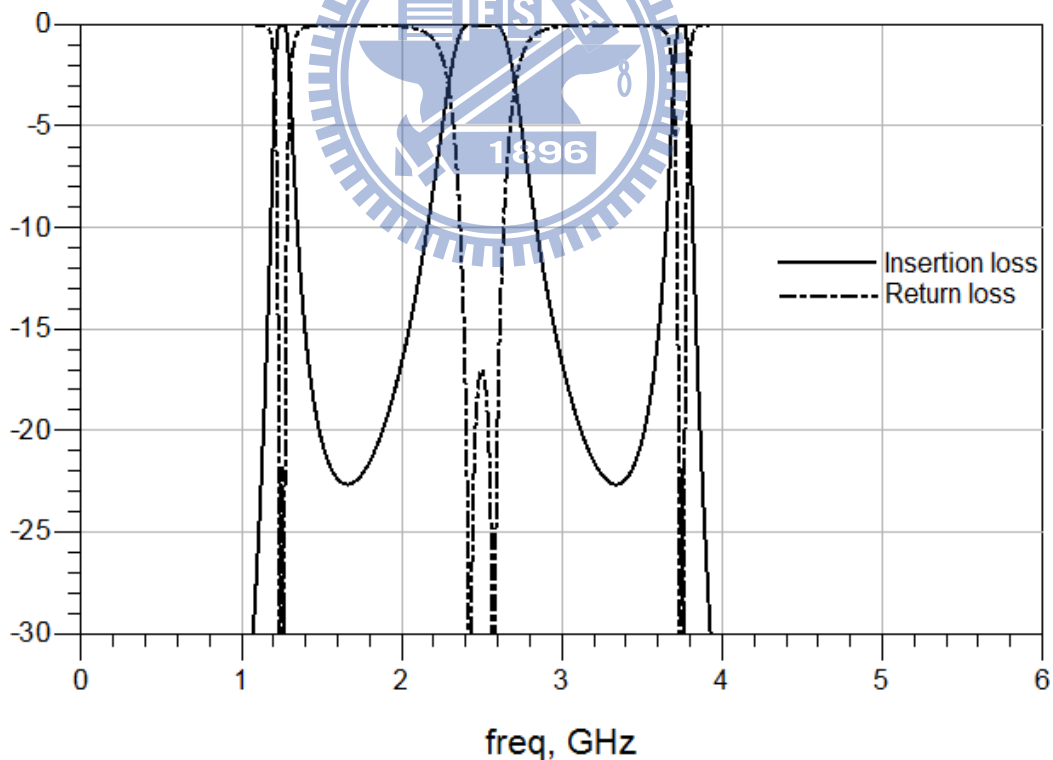


Figure 4.8 Simulated insertion loss and return loss the band-pass filter in figure 4.7

We use diodes to switch the mode of the filter. Since the forward resistance of the diode

is not 0, then  $Z_{in} = \frac{Z_0^2}{Z_L} \neq \infty$ . Therefore, we may take diode parameters into consideration and increase impedance to get better performance. Firstly, we consider the status of diode on as in figure 4.9.

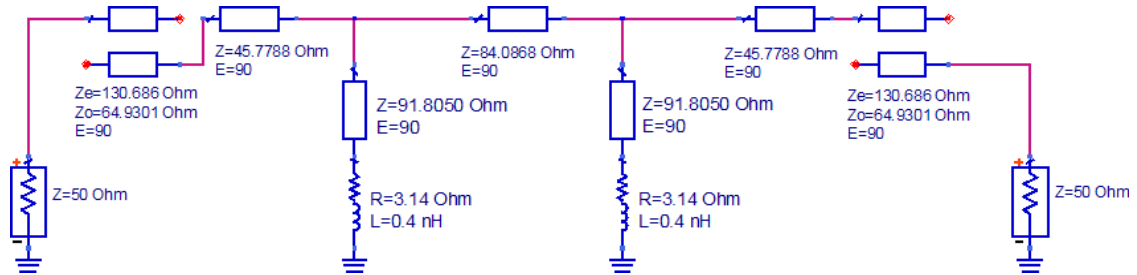


Figure 4.9 Band-pass filter of return loss 17dB, center frequency 2.5GHz, fractional bandwidth 15%

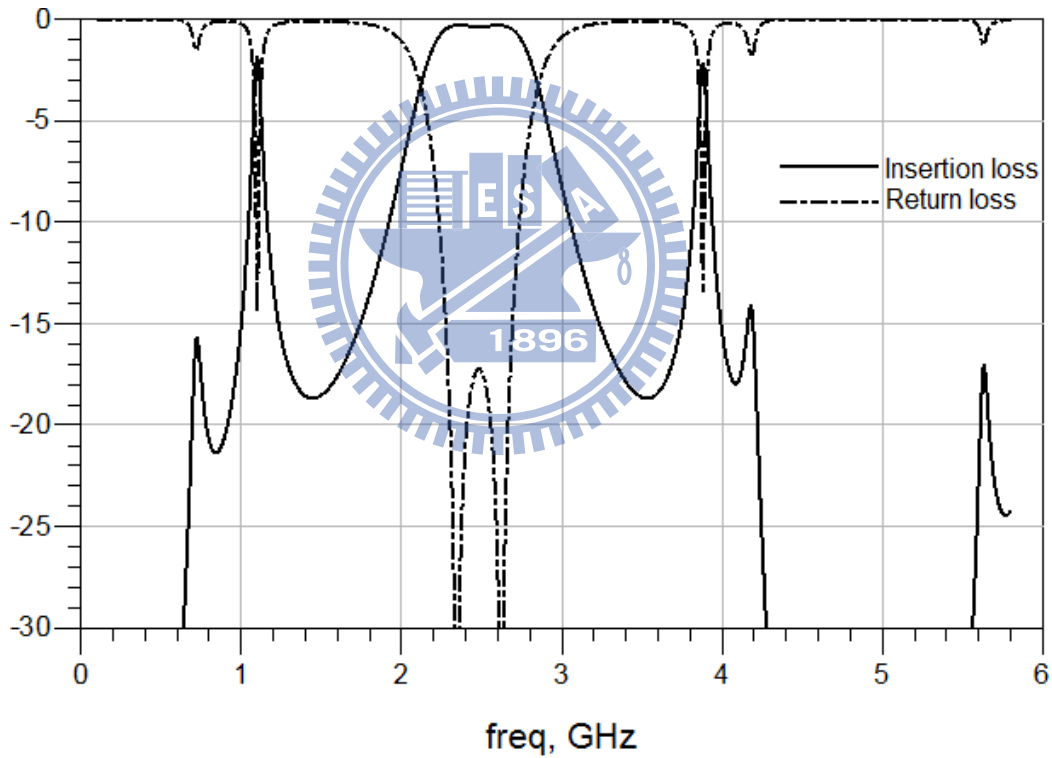


Figure 4.10 Simulated insertion loss and return loss of the band-pass filter in figure 4.9

As for diode on, we need to consider the effect of blocking capacitor for even mode.

The circuit is shown in figure 4.11.

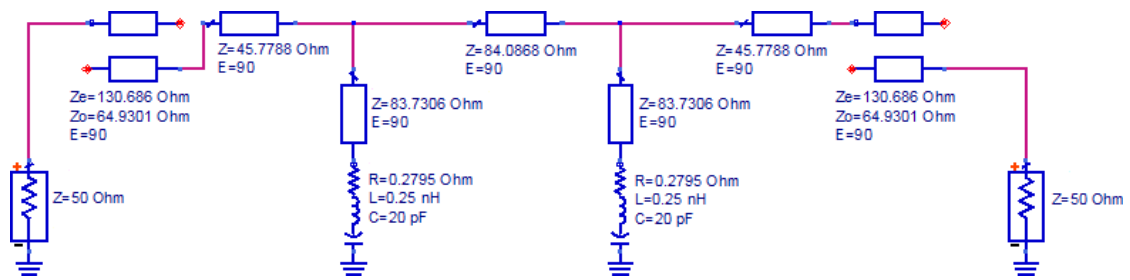


Figure 4.11 Band-pass filter of return loss 17dB, center frequency 2.5GHz, fractional bandwidth 15%

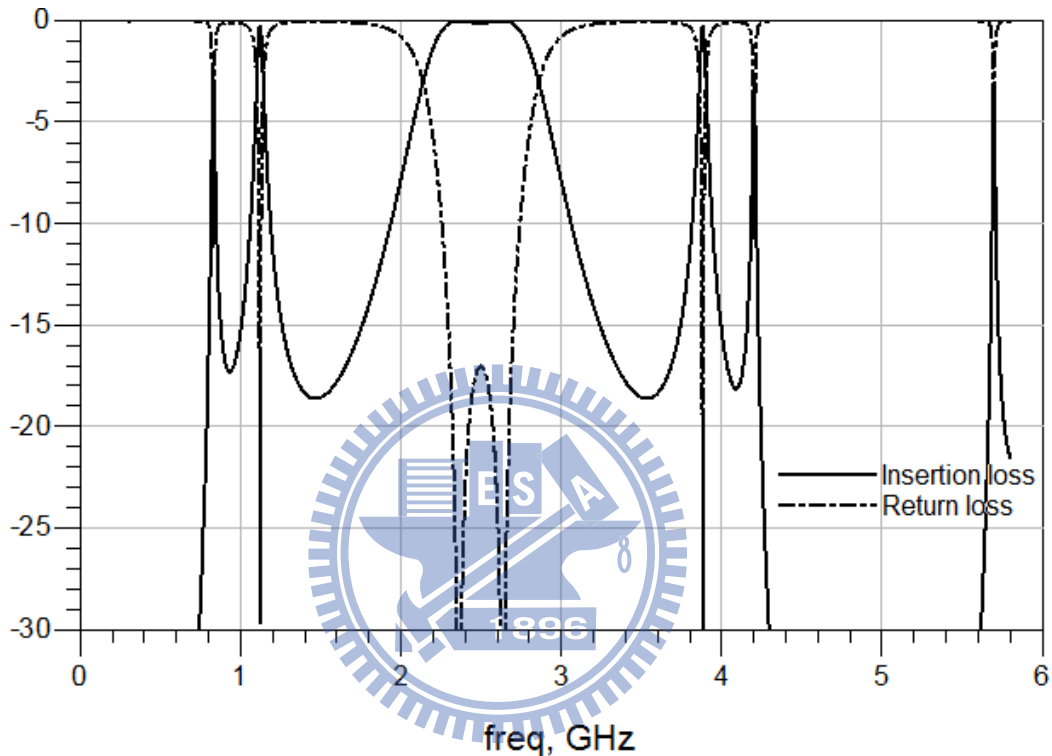


Figure 4.12 Simulated insertion loss and return loss of the band-pass filter in figure 4.11

### 4.3 Band-stop Filter

Figure 2.9 shows a band-stop filter. Since the parameters of the band-pass are fixed, we cannot change the band-stop filter design. We just need to find out a set of parameters to achieve the performance. The two pairs of coupled line in the middle only contribute limited performance variance to the band-pass filters. We may change the electrical length of the coupled lines as below. The return loss of the band-pass filter will degrade from 17dB to about 15dB, but we may get better bandwidth of the band-stop filter.

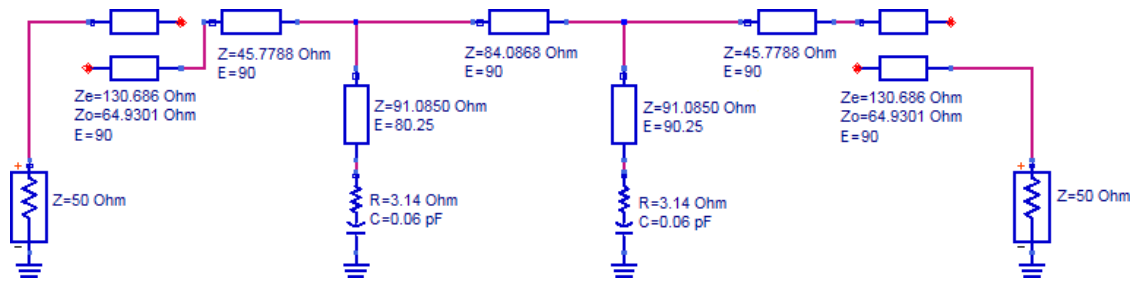


Figure 4.13 Band-stop filter under diode off, even mode, with insertion loss >35dB

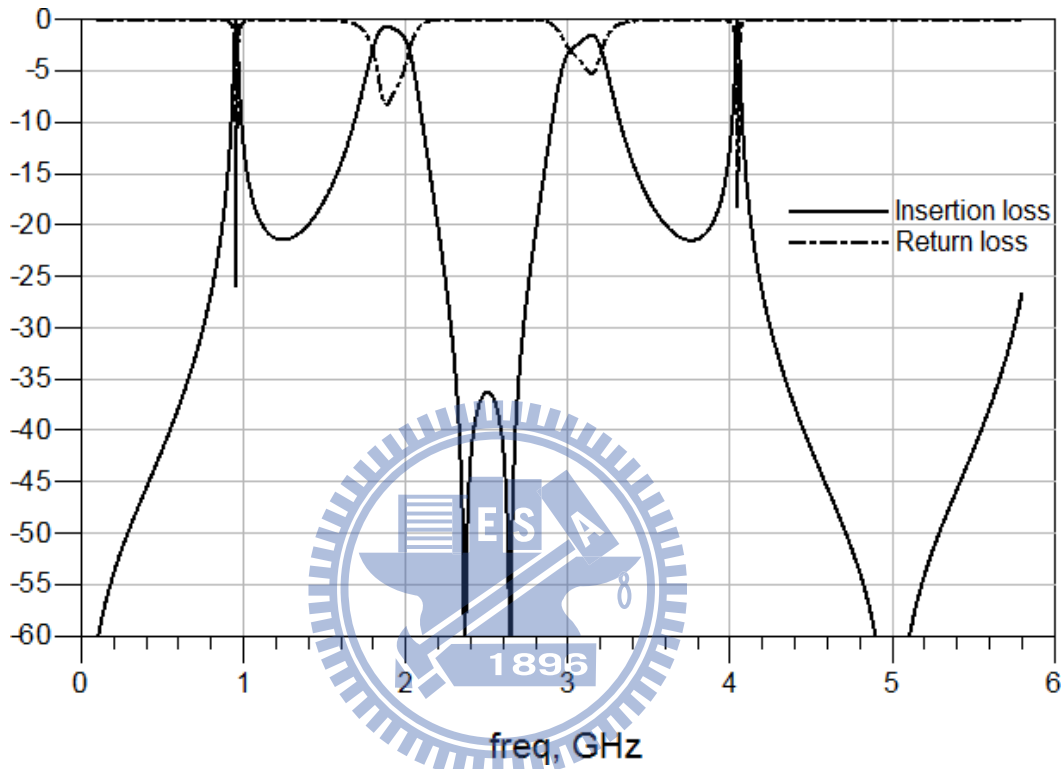


Figure 4.14 Simulated insertion loss and return loss of the band-stop filter in figure 4.13

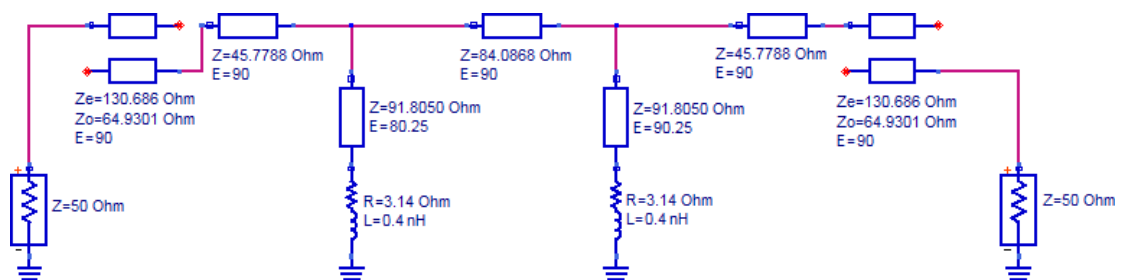


Figure 4.15 Band-pass filter under diode on, even mode, with return loss >15dB

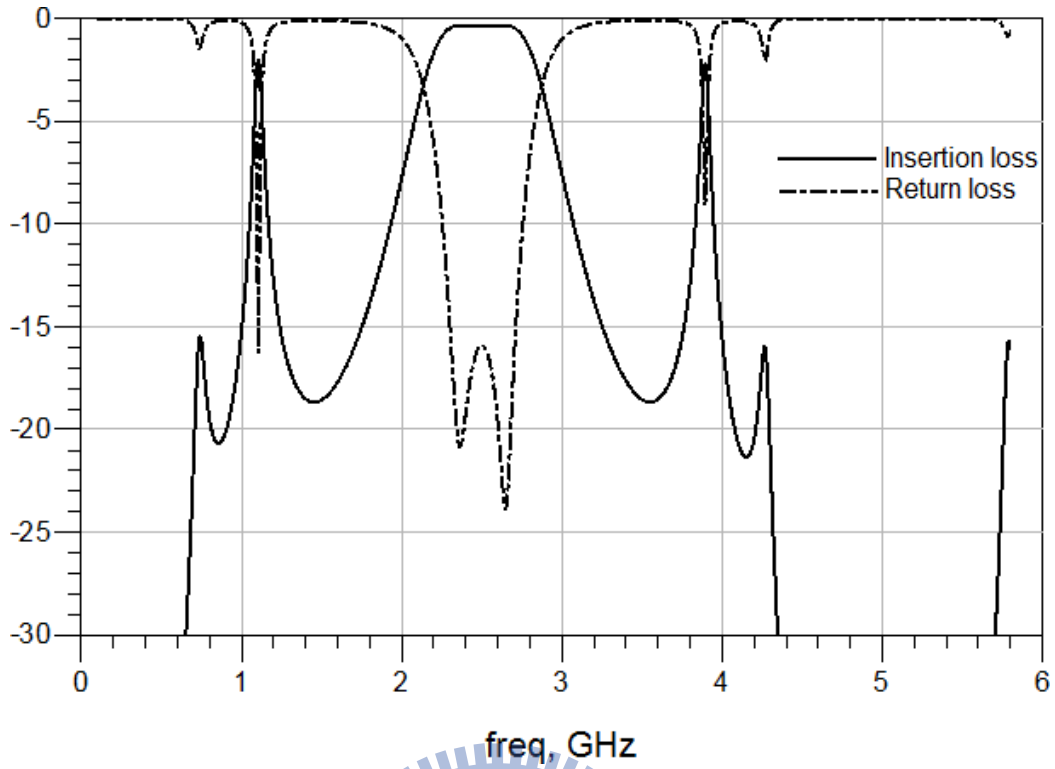


Figure 4.16 Simulated insertion loss and return loss of the band-pass filter in figure 4.15

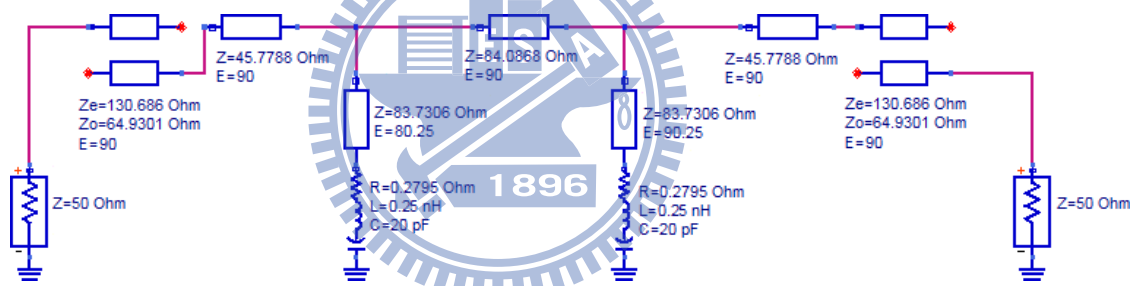


Figure 4.17 Band-pass filter under diode off, odd mode, with return loss >15dB



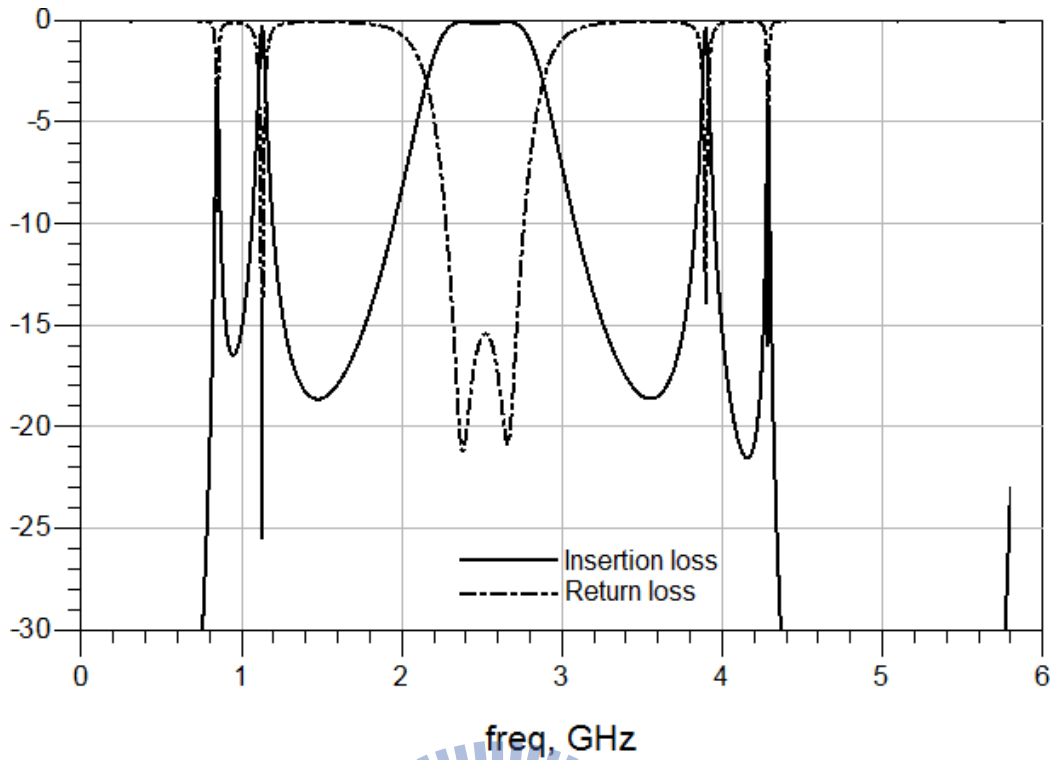


Figure 4.18 Simulated insertion loss and return loss of the band-pass filter in figure 4.17

#### 4.4 All-stop Filter

Below is the equivalent circuit of all-stop filter.

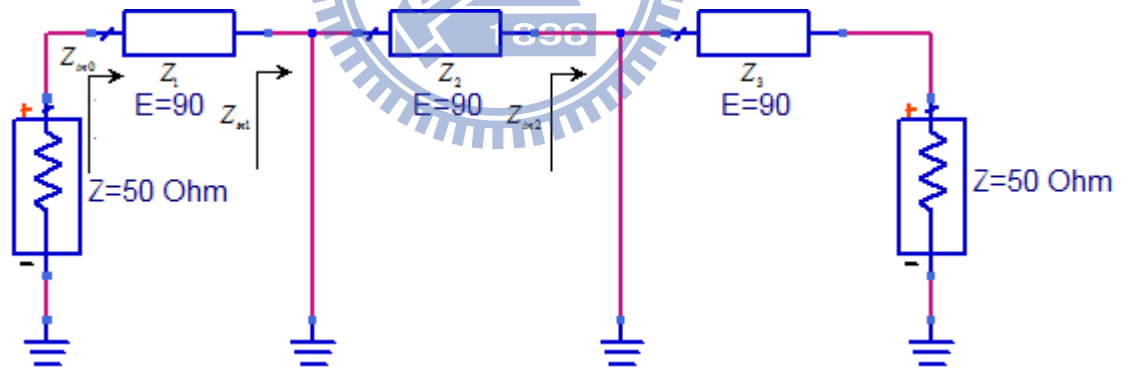


Figure 4.19 All-stop filter

$$Z_{in2} = 0\Omega // \frac{Z_3^2}{50\Omega} = 0\Omega \quad (130)$$

$$Z_{in1} = 0\Omega // \frac{Z_2^2}{Z_{in2}} = 0\Omega \quad (131)$$

$$Z_{in0} = \frac{Z_1^2}{Z_{in1}} = \infty \quad (132)$$

$$\Gamma = \frac{Z_{in0} - 50}{Z_{in0} + 50} = 1 \quad (133)$$

At the center frequency, all the incident power will be reflected. At the other frequency, the electrical length of each line segment will not be 90 degrees.

$$Z_{in0} = Z_1 \cdot \frac{Z_{in1} + jZ_1 \tan \theta}{Z_1 + jZ_{in1} \tan \theta} = jZ_1 \tan \theta \quad (134)$$

$$\Gamma = \frac{Z_{in0} - 50}{Z_{in0} + 50} = \frac{jZ_1 \tan \theta - 50}{jZ_1 \tan \theta + 50} = \frac{Z_1^2 \tan^2 \theta - 50^2 + j100Z_1 \tan \theta}{Z_1^2 \tan^2 \theta + 50^2} \quad (135)$$

If the circuit is symmetric, all of the incident power will be reflected by the short circuit.

In other word, it can be taken as an all-stop filter.

If we take capacitor and diode effect into consideration, the all-stop filter is as below, and the performance will be degraded as well.

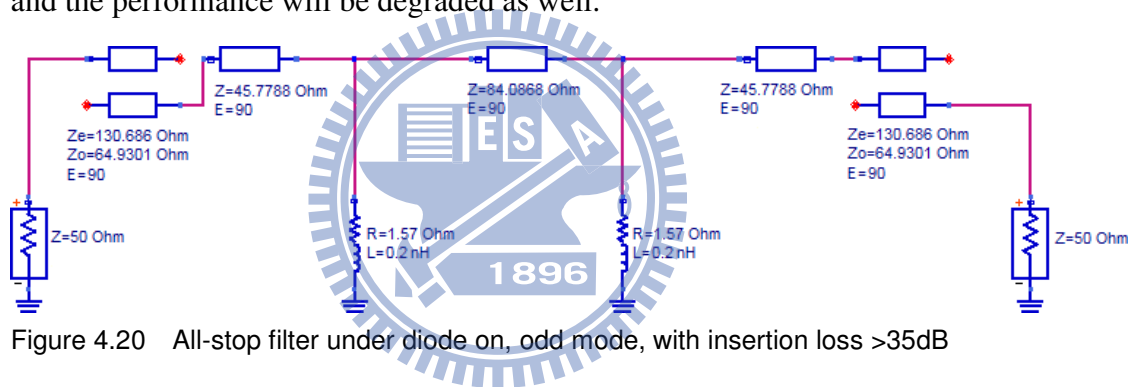


Figure 4.20 All-stop filter under diode on, odd mode, with insertion loss >35dB

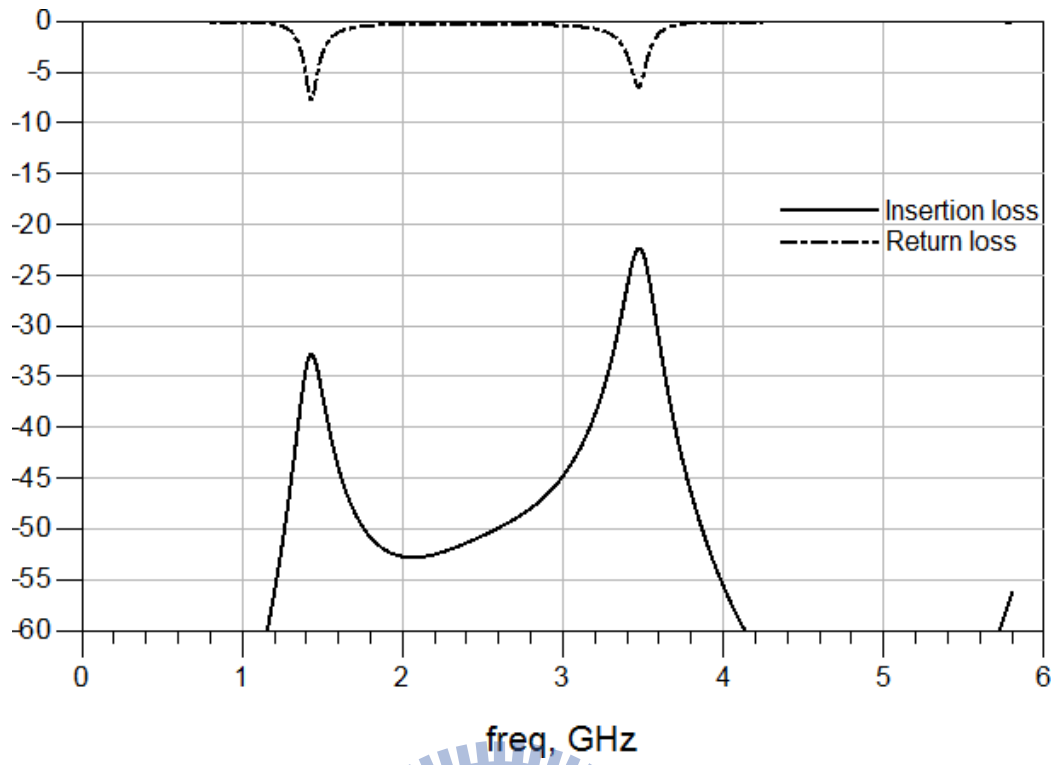


Figure 4.21 Simulated insertion loss and return loss of the all-pass filter in figure 4.20



## Chapter 5 Fabrication and Measurements

### 5.1 Circuit Fabrication

Figure 5.1 illustrates the photograph of the dual mode switch filter. Figure 5.2 and 5.3 illustrate the insertion loss and return loss measurement result. There is frequency shift effect, which will result in bandwidth degradation. The bandwidth (pass-band insertion loss  $<3\text{dB}$ , stop-band insertion loss  $>32.685\text{dB}$ , pass-band return loss  $>13.843\text{dB}$ , stop-band return loss  $<3\text{dB}$ ) is  $2.445\text{GHz}\sim 2.636\text{GHz}$ , which is about 7.64% fractional bandwidth.

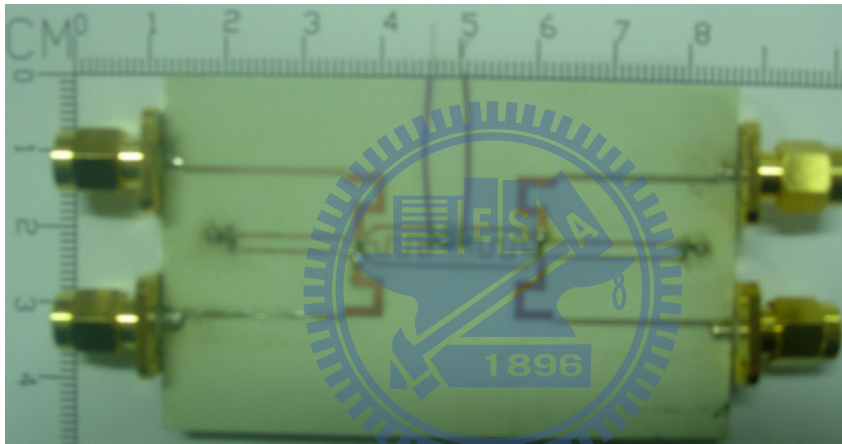


Figure 5.1 Photograph of the dual mode switch filter

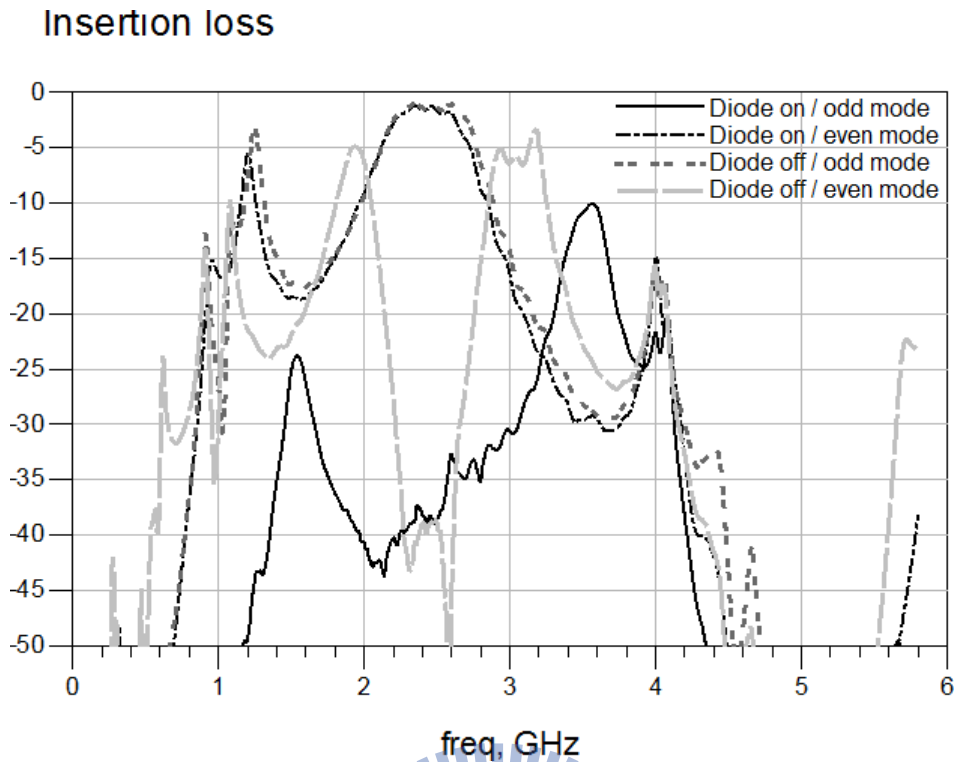


Figure 5.2 Measured insertion loss of dual mode switch filter

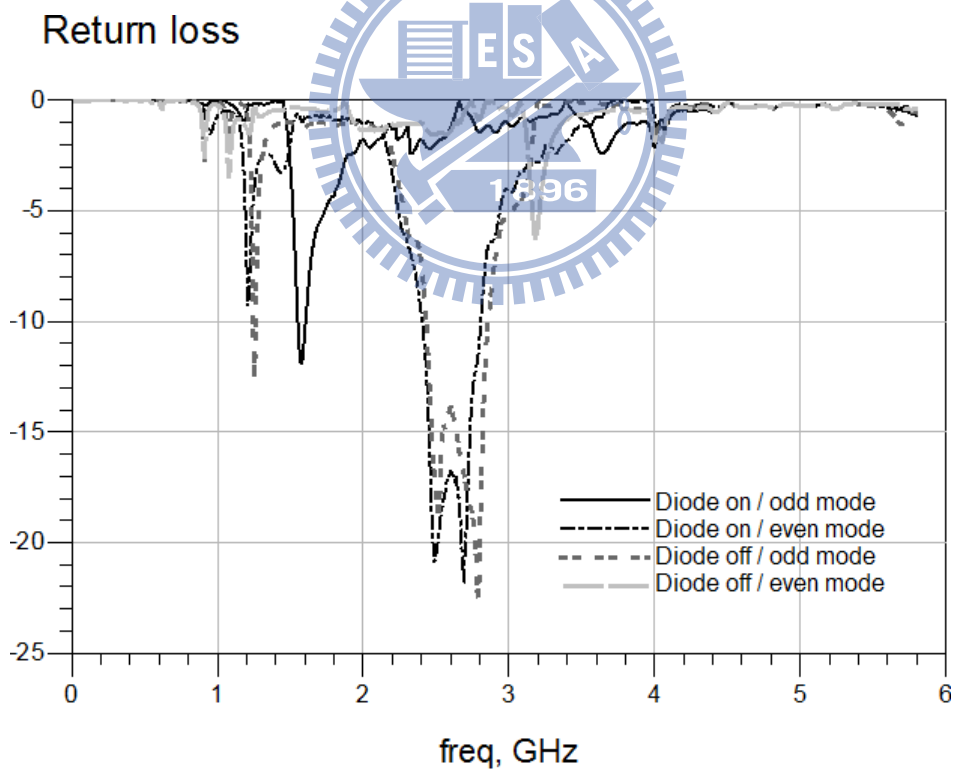


Figure 5.3 Measured return loss of dual mode switch filter

## 5.2 Measurement and 3D EM Simulation Correlation

Figure 5.4, 5.5, 5.6, 5.7 illustrate the correlation between measurement and 3D EM simulation. From the measurement result, the return loss measurement of the band-pass

filters are frequency up-shifted. The return loss measurement of the all-stop filter and band-stop filter match the 3D EM simulation. The insertion loss measurement of the band-pass filters, band-stop filter, and all-stop filter also match the 3D EM simulation.

### Diode on / odd mode (all-stop filter)

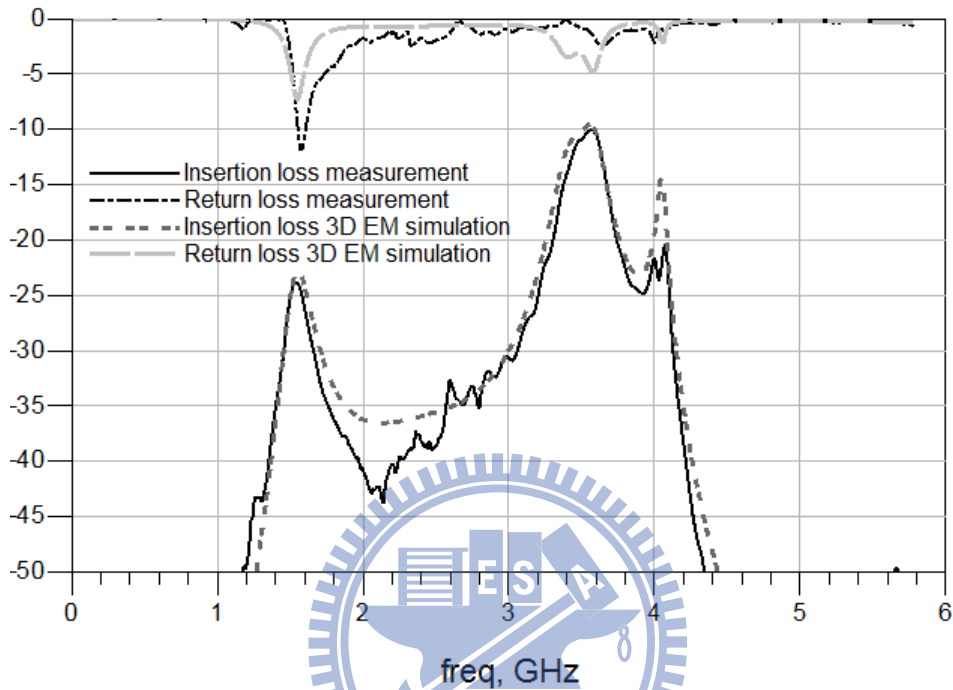


Figure 5.4 Measurement and 3D EM simulation correlation under diode on / odd mode

### Diode on / even mode (band-pass filter)

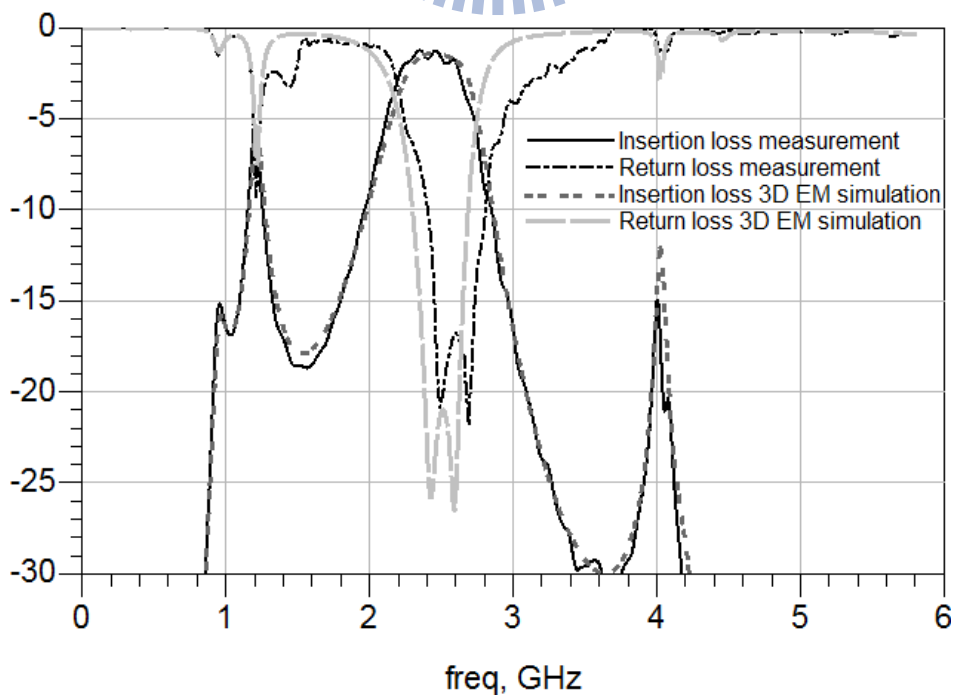


Figure 5.5 Measurement and 3D EM simulation correlation under diode on / even mode

### Diode off / odd mode (band-pass filter)

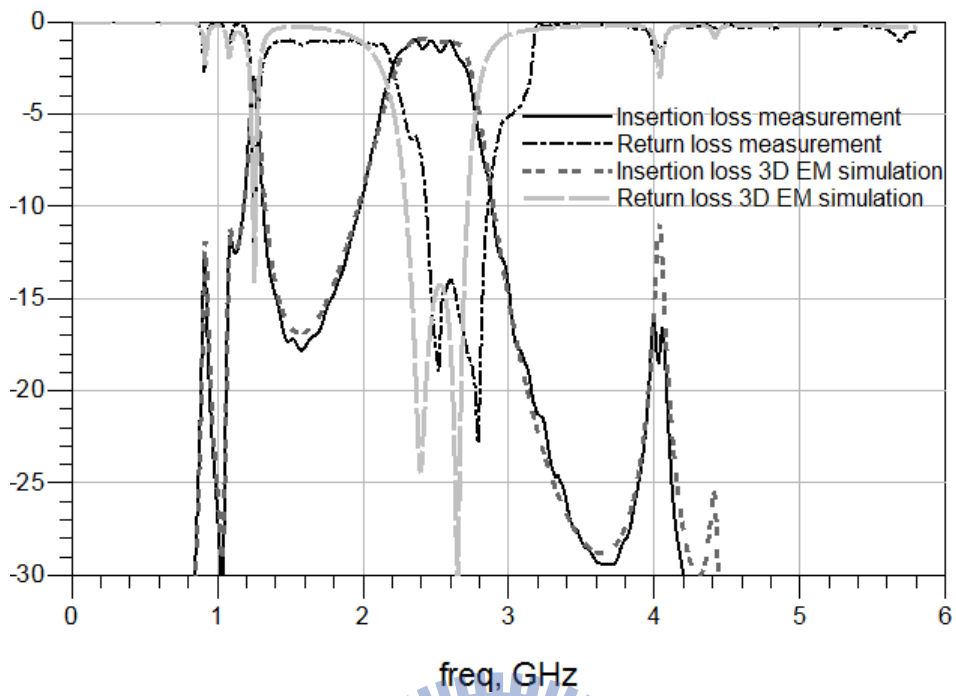


Figure 5.6 Measurement and 3D EM simulation correlation under diode off / odd mode

### Diode off / even mode (band-stop filter)

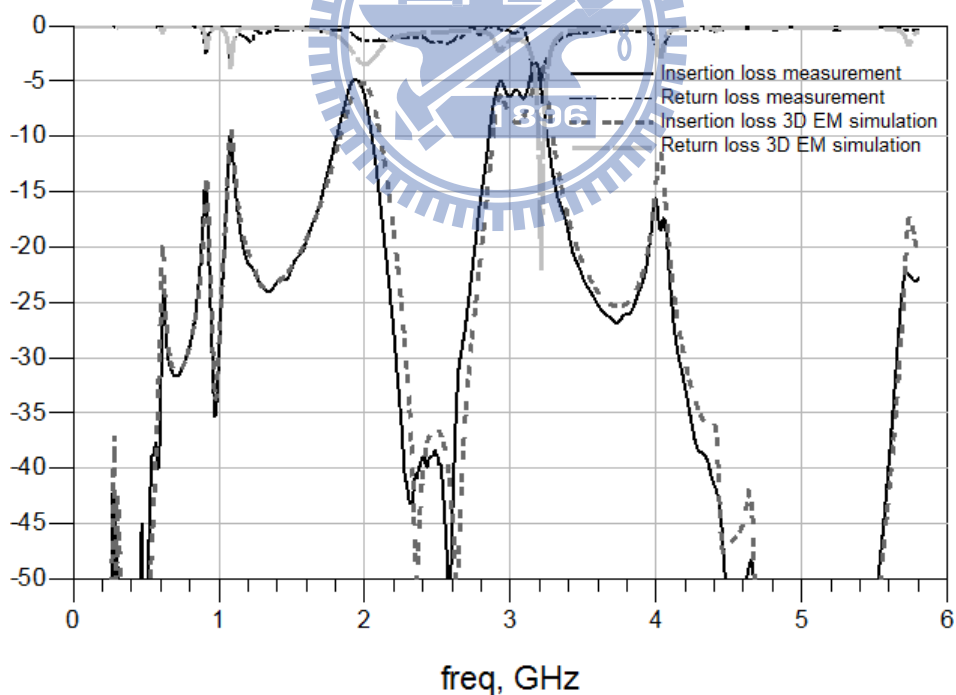


Figure 5.7 Measurement and 3D EM simulation correlation under diode off / even mode

## 5.3 Conclusion

From the measurement result, it is proved that dual-mode switch filter can work well at the center frequency. However, the circuits fabrication error and component variance

will impact the performance of the dual-mode switch filter. From the simulation result, the length  $lc2$  of the right half of the coupled line will impact the filter performance a lot. It is a critical to fine tune  $lc2$  length in manufacturing.

The circuit miniaturization is a topic of future works. The DC blocking coupled line plays a role of DC blocking and load impedance transformation. Theoretically, we may combine the DC blocking coupled line and the filter section 1. We need 3 sections of coupled lines to implement the second order band-pass filter. However, we may still need to fine tune the layout and check if there is any side effect in 3D EM simulation or circuit fabrication.





## References

- [1] David M. Pozar, *Microwave Engineering*, 3<sup>rd</sup> Edition, John Wiley & Sons, N.Y., 2005.
- [2] Christophe Caloz, and Tatsuo Itoh, *Electromagnetic Metamaterials*, John Wiley & Sons, 2005.
- [3] Hsin-Chia Lu and Tah-Hsiung Chu, “Multiport Scattering Matrix Using a Reduced-Port Network Analyzer“, *IEEE Transactions on Microwave Theory and Techniques*, Vol.51, No.5, May 2003
- [4] Rivlin T.J., *Chebyshev Polynomials*, John Wiley & Sons, N.Y., 1999.
- [5] George L. Matthæi, Leo Young, and E. M. T. Jones, *Microwave Filters, Impedance-Matching Networks, and Coupling Structures*, Artech House, M.A., 1980.

